Evidence of thermal-driven processes triggering the 2005-2014 unrest at Campi Flegrei caldera

Giovanni Chiodini[a,*], Jean Vandemeulebrouck[b,c], Stefano Caliro[a], Luca D'Auria[a], Prospero De Martino[a], Annarita Mangiacapra[a], Zaccaria Petrillo[a]

[a]Istituto Nazionale di Geofisica e Vulcanologia (INGV), Osservatorio Vesuviano, Via Diocleziano 328, Napoli, Italy.

[b]Université de Savoie, ISTerre, F-73376 Le Bourget du Lac, France.

[c]CNRS, ISTerre, F-73376 Le Bourget du Lac, France.

***Corresponding author: Giovanni Chiodini**

Istituto Nazionale di Geofisica e Vulcanologia (INGV),

Osservatorio Vesuviano,

Via Diocleziano 328, Napoli, Italy

Phone: +39-081-6108448

Fax: +39-081-6100811

E-mail: giovanni.chiodini@ingv.it

Abstract

An accelerating process of ground deformation that began 10 years ago is currently affecting the Campi Flegrei caldera. The deformation pattern is here explained with the overlapping of two processes: short time pulses that are caused by injection of magmatic fluids into the hydrothermal system; and a long time process of heating of the rock. The short pulses are highlighted by comparison of the residuals of ground deformation (fitted with an accelerating polynomial function) with the fumarolic CO_2/CH_4 and He/CH_4 ratios (which are good geochemical indicators of the arrival of magmatic gases). The two independent datasets show the same sequence of five peaks, with a delay of ~200 days of the geochemical signal with respect to the geodetic signal. The heating of the hydrothermal system, which parallels the long-period accelerating curve, is inferred by temperature–pressure gas geoindicators. Referring to a recent interpretation that relates variations in the fumarolic inert gas species to open system magma degassing, we infer that the heating is caused by enrichment in water of the magmatic fluids and by an increment in their flux. Heating of the rock caused by magmatic fluids can be a central factor in triggering unrest at calderas.

Keywords: Campi Flegrei caldera; hydrothermal system; ground deformation; magmatic fluids; caldera unrest.

1. Introduction

The trigger mechanism of unrest at active calderas is one of the most problematic issues of modern volcanology (Newhall and Dzurisin, 1988; Lowenstern et al., 2006; Troise et al., 2006; Gottsmann and Marti, 2008). In particular, magma displacement *versus* hydrothermal dynamics is one of the central questions for an understanding of the signals of several restless calderas on Earth, including, e.g., Yellowstone (Wicks et al., 2006; Lowenstern et al., 2006; Dzurisin et al., 2012;), Long Valley (Hill, 2006), Santorini (Parks et al., 2012), Nisyros (Chiodini et al., 2002), and Campi Flegrei. Here we focus on Campi Flegrei caldera (CFc), which is sited in the densely inhabited metropolitan area of Naples (southern Italy; Fig. 1, Napoli). Campi Flegrei caldera has recently given clear signs of potential reawakening (Chiodini et al., 2012) where long time series of geophysical and geochemical data are available. Throughout its history, CFc has alternated between phases of uplift and subsidence over a range of timescales (Rosi et al., 1983; Di Vito et al., 1999; Orsi et al., 2004; Morhange et al., 2006), and it showed evidence of decades-long inflation prior to the last magmatic eruption (the AD 1538 Monte Nuovo eruption; Dvorak and Mastrolorenzo, 1991).

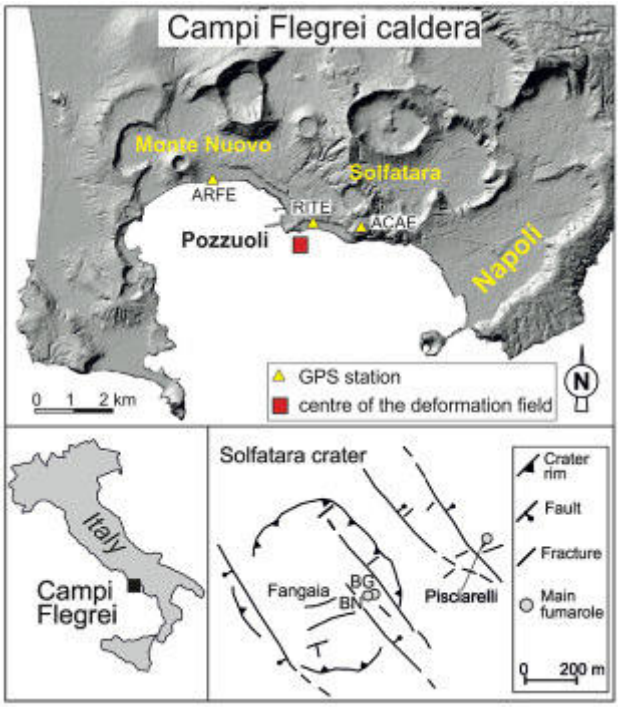

Figure 1. Location of Campi Flegrei caldera, Solfatara crater, and the main fumaroles. The map also shows the position of the CGPS stations referred to in the text, and the deformation field during 2005-2014.

The Monte Nuovo eruption was followed by a long period of subsidence, until the early 1950s, when inflation was resumed. This has culminating in two major uplift and seismic episodes ('bradyseisms'), which occurred in 1969-1972 and in 1982-1984, which

have shown a total vertical displacement of 3.8 ±0.2 m (Del Gaudio et al., 2010, and references cited therein). In 1982-1984, the maximum uplift of 1.8 m was accompanied by ~16,000 shallow earthquakes that affected CFc, which caused the partial evacuation of the heavily populated town of Pozzuoli (Barberi et al., 1984).

Since 1985, CFc has been slowly subsiding, which has been interrupted by a few minor uplift events. In 2005, there was new inflation, which accelerated and reached a maximum vertical displacement of about 23 cm by June 2014. This last stage was accompanied by weak seismicity, by a strong increase in fumarolic activity (Fig. 2), and by important compositional variations in the fumarolic effluents, which were interpreted as increased contributions from a magmatic source (Chiodini et al., 2012, and references therein). For instance, these phenomena induced the Italian Civil Defence to change the state of Campi Flegrei from the green level (quiet) to the yellow level (scientific attention).

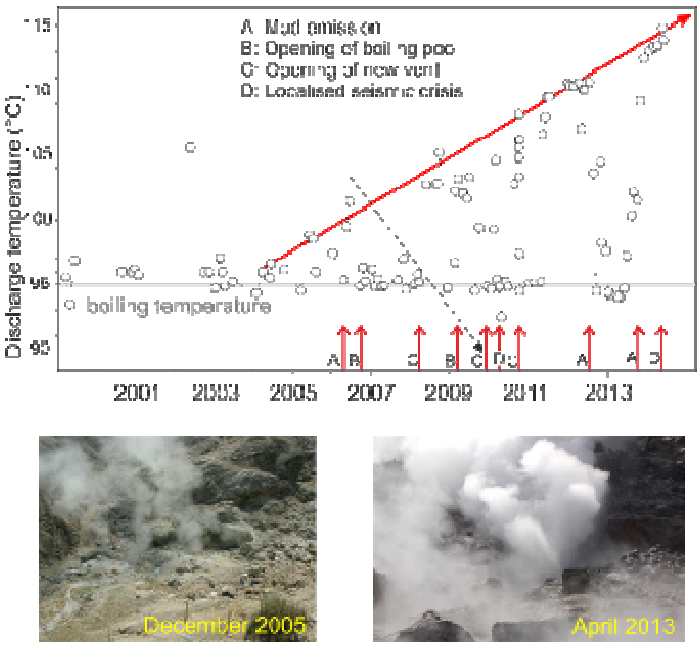

Figure 2. Time series of discharge temperatures at Pisciarelli fumarole, and chronogram of localized phenomena that have affected the hydrothermal site (red arrow). The two pictures highlight the strong increase in fumarolic flow rate from 2005 to 2013.

The first part of this study aims to illustrate the main features of this hydrothermal system. Then, we investigate the possible causes of the new unrest at CFc, by comparison of the long time series of the Solfatara fumarole composition with ground deformation data obtained from the continuous GPS network (De Martino et al., 2014).

1.1 The hydrothermal system that feeds Solfatara

A conceptual geochemical model of the hydrothermal system that feeds the fumaroles of Solfatara based on fumarole effluent composition was first proposed by Cioni et al. (1984), and then refined by Cioni et al. (1989), Chiodini et al. (1996), Chiodini and Marini (1998), Chiodini et al. (2001, 2010), and Caliro et al. (2007). According to the most comprehensive work of Caliro et al. (2007), hot gases separate from the magma at depth, ascend toward the surface, mix with boiling meteoric water to form a gas plume that feeds fumaroles and diffuse soil degassing at Solfatara. This geochemical interpretation has been supported by numerous physical–numerical simulations that have been published in the last 10 years (Chiodini et al., 2003, 2012; Todesco et al., 2003; Todesco 2009; Rinaldi et al., 2010; Petrillo et al., 2013). All of the models have consisted of injection at depth beneath Solfatara crater (1.5-2.5 km) of a hot CO_2-water mixture, where its flux is constrained by the surface hydrothermal flux measured at Solfatara. All of the simulations have been performed with the TOUGH2 code (Pruess, 1991) under steady-state conditions, and they have returned the presence of a gas plume that vertically connects the deep injection zone to the surface.

Together with geochemical interpretations and simulation results, other independent data highlight the presence of a gas plume in the subsoil of Solfatara crater:

- The total CO_2 release from diffuse degassing processes at Solfatara and its surroundings (~1.4 km^2; Fig. 3a) was estimated at 1000 t/d to 1500 t/d from 1998 to 2010 (Chiodini et al., 2010). In addition, recent measurements of gas flux from the three main fumaroles of Solfatara that were performed in January 2013 indicated a total CO_2 output of up to ~600 t/d (Aiuppa et al., 2013). The total CO_2 flux of 1500 t/d to 2000 t/d was obtained by summing the fumarole fluxes and the diffuse emission, and this has to be considered as a minimum estimation of the total hydrothermal CO_2 output, because it does not consider the flux of the numerous smaller fumarolic discharges that have never been measured. Such high hydrothermal CO_2 flux is more compatible with the presence in the subsoil of a large zone where there is a gas phase (i.e., the gas plume), rather than with a boiling process of a liquid, which would require unreasonable amounts of boiling water. For example, at Yellowstone, high diffuse CO_2 fluxes of the same magnitude as at Solfatara (i.e., ~kg m^{-2} d^{-1}), are normally found in vapor-dominated hydrothermal areas (i.e., acid-sulfate areas), while relatively low diffuse CO_2 fluxes are observed in areas that are dominated by thermal liquid discharges (e.g., alkaline-chloride areas) (Werner and Brantley, 2003).

- At Solfatara, the aquifer is anomalously high for both the water table height (Fig. 3b) and the water temperature (Fig. 3c), with temperatures up to boiling point (Petrillo et al., 2013). These anomalies are due to the large amounts of condensates, which are of the order of thousands of tons per day, and which locally recharge and heat the groundwater system (Bruno et al., 2007; Petrillo et al, 2013). The height of the water level indicates that a pressurized gas plume sustains the aquifer here. Similar observations of aquifers saturated with hot water condensing from an underlying gas reservoir have been reported for vapor-saturated hydrothermal systems in Yellowstone (Zohdy et al., 1973) and at Waimangu, New Zealand (Legaz et al., 2009).

- The S-wave seismic velocity (V_S) models (data from Battaglia et al., 2008; Zollo et al., 2006; Fig. 3d) clearly delineate a vertical, roughly cylindrical, high-*Vs* structure that extends from the surface close to Solfatara crater, down to at least 1.5 km. This *Vs* anomaly is unique in the shallower part of CFc, and it can be attributed to the presence of gas instead of liquid, as suggested by laboratory measurements of *Vs* in dry samples of CFc tuffs, which are systematically 10% to 50% higher than the same samples saturated with liquid (Giberti et al., 2006). This vertical structure (Fig. 3d, inset) represents an easy way to transfer up-flowing hydrothermal gases that cause the evident surface anomalies in the gas flux, temperature and water-table level. The deep source of this hydrothermal gas plume might be the area of anomalously low *Vp/Vs* ratio, the roof of which is located 4 km below the city of Pozzuoli, which has been interpreted as a high fluid-compressibility (gas-saturated) rock formation (Vanorio et al., 2005).
- The geodetic imaging of InSAR data (D'Auria et al., 2012) reveals that during the 2006-2007 uplift episode, the ground deformation source below the Solfatara-Pisciarelli area had a roughly cylindrical shape, with a height of about 2 km and a radius of about 200 m. This source inflated in Oct. 2006, and deflated at the end of 2007. The onset of the inflation coincided with a seismic swarm of long-period events located underneath Solfatara. The inversion of the data showed the upward migration of fluid batches within this source.

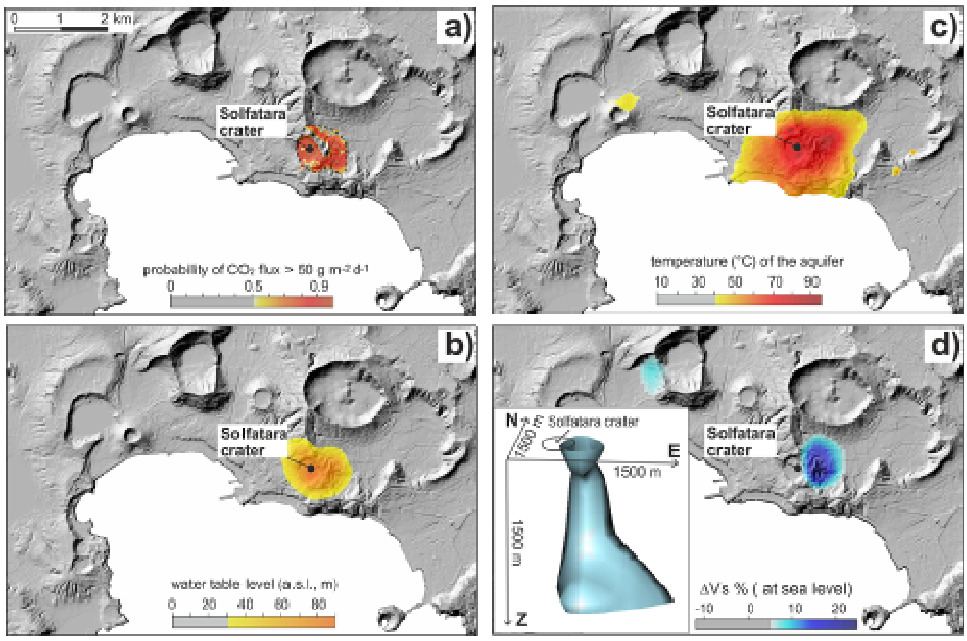

Figure 3. Main anomalies that characterize Solfatara crater and its surroundings: (a) soil-diffuse fluxes of CO_2; (b) height of the water table; (c) groundwater temperatures; and (d) anomalies in *Vs* velocities at sea level. The anomalies refer to the percent variations with respect to the mean value at each depth. The inset in (d) shows the volume containing anomalies of greater than 18%. The spatial coincidence among the different anomalies is caused by the presence of a gas plume in the subsoil of the area.

In summary, the main features of the hydrothermal system that feeds the Solfatara fumaroles are illustrated in Figure 4.

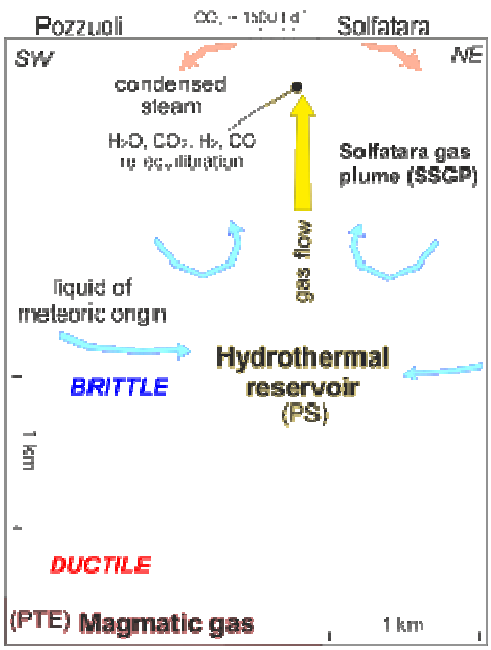

Figure 4. Conceptual model of the hydrothermal system feeding the Solfatara fumaroles. PTE and pressurized spheroid (PS) refer to the sources of the ground deformation that is active at CFc, according to Amoruso et al. (2014a,b).

The system consists of: (i) a deep zone of gas accumulation (Fig. 4, 'magmatic gas') which is located at ~4 km in depth (Vanorio et al., 2005), and which supplies hot gas to the system. In this zone, the presence of a small batch of magma has been hypothesized (De Siena et al., 2010); (ii) a shallower reservoir (~2 km in depth), where magmatic fluids mix and vaporize liquid of meteoric origin that forms the Solfatara gas plume. This scheme was previously inferred from geochemical interpretations (Caliro et al. 2007, 2014; Chiodini et al. 2012), and it was also supported by the most recent inversion of the ground deformation data for the 1982-2013 period (Amoruso et al., 2014a,b). The observed deformation would be controlled by pressure changes in two distinct sources: a pressurized triaxial ellipsoid (PTE), oriented NW-SE and centred at about 4 km in depth below Pozzuoli; and a pressurized spheroid (PS) located at ~2 km in depth below Solfatara crater. The PTE and PS are coincident with the deeper and shallower parts of the hydrothermal system (Fig. 4).

2. Materials and methods

2.1 Datasets used

In the following sections we will mainly refer to:

- the composition of the Solfatara fumaroles (BG 161°C ± 2.7°C; BN 146.0 ± 2.0°C, Fig. 1), which are sampled monthly and analyzed in the framework of the volcanic surveillance of CFc. The chemical species routinely determined are H_2O, CO_2, H_2S, H_2, N_2, CH_4, He and CO (in order of decreasing concentrations), which have shown large compositional variations over time (Chiodini et al., 2010). The entire dataset, which consists of 446 previously published samples and 83 new samples, analytical methods, and errors accompany this study, in the electronic Annex.
- the dataset of the CFc surface deformation detected by continuous GPS stations (CGPS), as recently published in an open-access database (De Martino et al., 2014).
- the vertical maximum displacement recorded by high-precision leveling surveys for the 1982-2003 period (Del Gaudio et al., 2010).

2.2 Gas equilibria models

In this study, we investigated the gas equilibria within the H_2O-CO_2-H_2-CO gas system, modifying the approach described in Chiodini and Marini (1998) in order both to derive gas geoindicators independent on the occurrence of condensation processes and to estimate the fraction of water removed or added in secondary processes. The equilibrium temperature and pressure were derived based on the following assumptions:

(a) The H_2 and CO fugacities are controlled by the dissociation of H_2O and CO_2 according to:

$$CO_2 = CO + ½ O_2 \quad (1),$$

$$H_2O = H_2 + ½ O_2 \quad (2);$$

(b) The equimolar ratios between the molar fractions are equal to the ratios between the fugacities ($X_i/X_j \approx f_i/f_j$), an assumption that is generally valid in the typical pressure–temperature range of hydrothermal systems;

(c) The water fugacity is fixed by the coexistence of liquid and vapor phases;

(d) The gases equilibrate in the vapor phase. This assumption is not obvious, because in most cases the fumaroles are fed by boiling liquid rather than from zones of equilibrated vapor. However, at Solfatara, there is abundant evidence for a large gas plume where reactive gas species equilibrate (see section 2);

(e) Redox conditions are controlled for both the H_2-H_2O and CO-CO_2 couples by a unique f_{O2}-T function. In particular, we applied the function of D'Amore and Panichi (1980) ($\log f_{O2} = 8.20 - 23643/T$, where T is the temperature, expressed in Kelvin), which according to Chiodini and Marini (1998) is the function that generally better describes redox conditions, among the different functions proposed for hydrothermal environments.

With these assumptions, we derived the following geothermometric and geobarometric functions:

$$T = 3238/[1.115 - \mathrm{Log}(CO/CO_2)] \quad (3);$$

$$\mathrm{Log}\ P_{H2O} = 5.510 - 2048/T, \text{ (Giggenbach 1980)} \quad (4);$$

$$\mathrm{Log}\ P_{CO2} = 3.573 - \log(H_2/CO) - 46/T \text{ (Chiodini and Cioni, 1989)} \quad (5),$$

where the estimated values depend on the measured ratios of the noncondensable gases (i.e., CO/CO_2 and H_2/CO).

The fraction of the water removed or added in secondary processes was computed by comparing the ratio between the equilibrium P_{H2O} and P_{CO2} $[(H_2O/CO_2)_{eq}]$ with the analytical fumarolic ratio of H_2O/CO_2. Theoretically, these two values should be almost equal if the gas moves from the equilibration zone to the fumarolic discharge without water and CO_2 removal or addition. Assuming that CO_2 removal or addition is negligible, the H_2O and CO_2 mass balance between the equilibration zone (subscript *eq*) and the fumarolic discharge (subscript *fu*) can be expressed by the simple relations:

$$CO_{2,eq} = CO_{2,fu} \quad (6)$$

$$H_2O_{eq} = H_2O_{fu} + f\,H_2O_{eq} \quad (7)$$

where f is the fraction of the water removed (sign +, condensation) or added (sign -, addition of water) in secondary processes, and is computable. Combining this with Equations (1) and (2), we get:

$$f = [(H_2O/CO_2)_{eq} - (H_2O/CO_2)_{fu}] / (H_2O/CO_2)_{eq} \quad (8).$$

3. Results and discussions

3.1 The pattern of the 2005-2014 ground deformation and geochemical signals

The CGPS data (De Martino et al., 2014) show that since 2005, the entire CFc has uplifted and expanded with spatially varying amplitudes, but following a similar accelerating process (De Martino et al., 2014: Figs. 2-4). The maximum vertical displacement was measured at the RITE CGPS station, the station that is closest to the center of the deformation field (Fig. 1); this uplifted by ~23 cm from April 2005 to June 2014, following an accelerating trend. The same pattern has also characterized the horizontal displacement of CFc, as shown in Figure 5a by the time series of the baseline length variations between the ACAE and ARFE CGPS stations, which have moved toward the ENE and WNW, respectively. In the following, we will rely on the ACAE-ARFE baseline time series, as this has been less affected by atmospheric effects than the vertical time series of the RITE station. Inspection of the curve shown in Figure 6a suggests that there has been overlapping of a general trend of expansion

with short periods of dilatation pulses (or uplifting), two of which were particularly intense and which commenced in 2006 and 2012. To derive a general long-term trend of the deformation, we fitted the CGPS measurements to a third-order polynomial equation applied to the points less affected by these pulses (i.e., the relative minima of the curve; Fig. 5a, black dots). The residuals of the observed data with respect to the curve fitting clearly show the two anomalous mini-uplift episodes of 2006-2007 and 2012-2013, along with a series of less-intense ground-deformation episodes. On the whole, the residuals of the deformation closely resemble the geochemical data collected at Solfatara fumaroles (Fig. 5b, c).

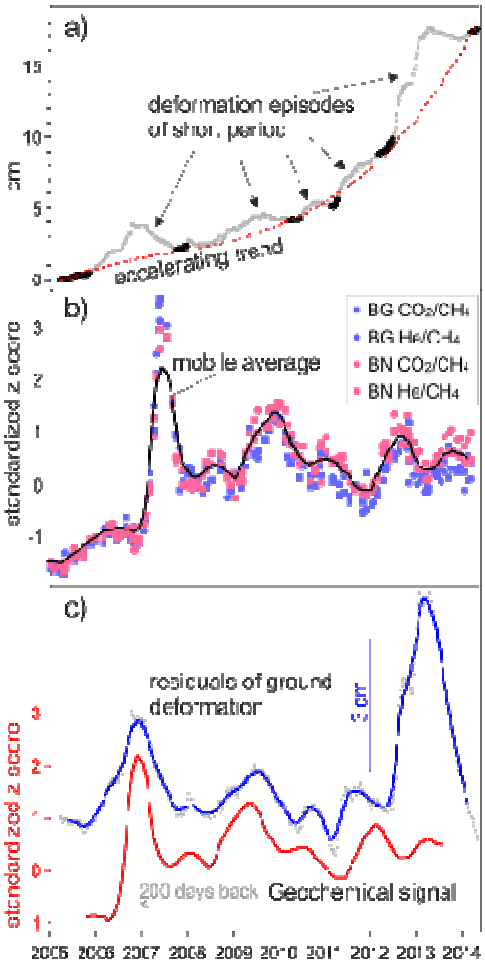

Figure 5. Comparison between ground deformation and geochemical signals. a) 2005-2014 baseline length variation between the ACAE and ARFE CGPS stations (gray dots, see Fig. 1 for the location of ACAE and ARFE). The data used for the derivation of the 'accelerating trend' curve are reported as black dots (see the text for further explanations); b) measured CO_2/CH_4 and He/CH_4 ratios at fumaroles BG and BN. In order to compare the different signals the measured data were normalized (standardized z-score) by removing the mean and dividing by their standard deviation (2004-2014 period). The 4 months mobile average of all the geochemical data (red curve) shifted backwards by 200 days is compared in panel (c) with the 4 months mobile average of the ground displacement residual (see panel a).

At the Solfatara fumaroles, the sharp increase in the proportion of the magmatic component over relatively short periods, i.e., of a few months to a year, was interpreted as resulting from magmatic fluid injections into the hydrothermal system (Chiodini et al., 2012). During these

episodes, the CH_4 content of the fumaroles decreased, due to the low CH_4 content of the magmatic fluids, and possibly also because the relatively high and transient oxidizing conditions during magmatic fluid injection can prevent the formation of CH_4 in the hydrothermal environment (Chiodini, 2009). On the contrary, other gases of prevalent magmatic origin, such as CO_2 and He, can increase their relative contents, making their ratio with CH_4 a good indicator of an increasing proportion of the magmatic component. Therefore, the five peaks that affected the CO_2/CH_4 and He/CH_4 ratios of BG and BN fumaroles in 2007, 2008, 2009-10, 2011, 2012 (Fig. 6b), which were each of about 1 year in duration, correspond to periods of magmatic fluid enrichment in the Solfatara fumaroles. These geochemical pulses closely repeat the same sequence of six minima and five maxima that are highlighted by the residuals of the displacements, the main difference being a time lag of about 200 days between the ground deformation and the geochemical signals (Fig. 6c).

Excluding an improbable fortuity, this correlation between two truly independent datasets can be explained by episodes of pressurization in the deeper parts of the hydrothermal system, followed by pulsed inputs of magmatic fluids into the system that feeds the Solfatara fumaroles. The delay between the two signals would represent the transfer time of the magmatic fluids from the input zone (i.e., Fig. 5, PTE reservoir) to the fumarolic discharge areas. Only the last important deformation event (Fig. 6c, 2012-2013) does not correspond to a geochemical peak of comparable intensity. It is worth noting that at that time (i.e., autumn 2012) the earthquakes hypocenters moved from below Solfatara (at a depth of ~1-2 km) to 2 km to the west, at greater depths (2-4 km), which would suggest that a similar fluid transfer process affected another zone of CFc.

These evident episodes of gas pressurization and magmatic fluid transfer occur concurrently with the accelerating trend of deformation (Fig. 6a) the origin of which is discussed in the next sections.

3.2 Evidence of heating of the Solfatara hydrothermal system during 2005-2014

During the 2005-2014 period of accelerating deformation (Fig. 5), the CO/CO_2 ratio of the main fumaroles also showed a clear increase, from ~3×10^{-6} in 2005, to ~5×10^{-6} in 2014 (Fig. 6a). This similarity between the ground deformation and the CO/CO_2 ratio is relevant because CO is the most sensitive species to temperature among all of the fumarolic reactive gas species (Chiodini and Marini, 1998). Due to its relatively fast kinetics for equilibration with CO_2 (Chiodini and Marini, 1998), the CO increase would appear to be caused by heating of the shallower parts of the Solfatara gas plume (Fig. 4). For the same period, the CH_4, which is

a much slower species to react (Giggenbach, 1987) and which is formed in deeper parts of the hydrothermal system (Caliro et al., 2007), shows a clear general decreasing trend (Fig. 6b, CH_4/CO_2 ratio) that can be explained by the ingress of oxidizing magmatic fluids into the deeper parts of the hydrothermal system and, in turn, by a temperature increase that hinders CH_4 formation. Therefore, CO and CH_4 qualitatively indicate a temperature increase for the entire CFc hydrothermal system.

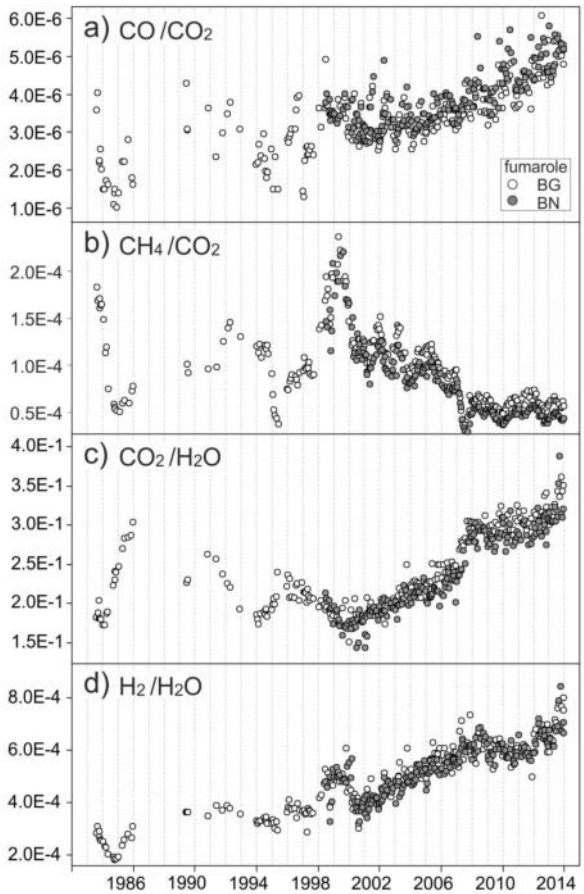

Figure 6. Time series of (a) CO/CO_2, (b) CH_4/CO_2, (c) CO_2/H_2O, and (d) H_2/H_2O molar ratios at the Bocca Grande (BG) and Bocca Nuova (BN) fumaroles.

This heating of the system appears to be caused by the increment in the flux of the magmatic fluids that enter the hydrothermal system, which results in the pulsed anomalies depicted in Figure 5c. In particular, Chiodini et al. (2012) estimated that the total injected fluid masses associated with each of these events are of the same order of magnitude (Mega ton) as those emitted during small to medium-sized volcanic eruptions, and that their cumulative curve highlights increasing activity during the period of accelerating deformation. According to the results of physical simulations (Todesco, 2009), the increment in the flux of the deep hot fluids would cause water vapor condensation within and at the border of the gas plume, and in turn, heating of the rock by the latent heat release during condensation.

The condensation of the steam might be one of the main causes of the continuous increase in noncondensable gases in fumaroles (e.g., Fig. 6c, CO_2/H_2O ratio), a process that has been of particular note in recent years. The occurrence of an ongoing process of condensation-induced heating is also suggested by repeated episodes of mud emissions, and by the formation of boiling pools of condensates at the Pisciarelli site (Fig. 1); these started in 2004, and they have been accompanied by a progressive increase in the discharge temperature of the main vent, from 95 °C to 96 °C in 2004, to 115 °C in 2014 (Fig. 2; Chiodini et al., 2011).

The important processes of condensation at the Solfatara system are highlighted by the complex electrical resistivity structure of the first 100 m below Solfatara crater, which shows that the resistive gas bodies below the fumaroles are overlain by conductive descending bodies of liquid condensates (Byrdina et al., 2014). Furthermore, the electrical resistivity image shows an ascending column of condensates that emerge at the Fangaia site (Fig. 1), which supports the occurrence of deep processes of condensation within the buried Solfatara gas plume.

Previous studies of gas-geoindicators at Solfatara (Chiodini et al., 2011, and references therein) have assumed that the measured H_2O-CO_2-H_2-CO fumarolic concentrations are fully representative of their equilibrium compositions, an assumption that will not be valid if water vapor condensation is occurring. To derive gas-geoindicators of the temperatures and pressures based on the ratios among the noncondensable gas species, which are consequently not affected by the occurrence of steam condensation, we now select as an alternative constraint the redox conditions that are fixed by a typical hydrothermal buffer. This revised method (see section 2.2) allows the estimation of the temperatures and the fractions of the water (*f*) removed or added in secondary processes, such as condensation or addition of water during the transfer of the vapor from the equilibration zone to the fumaroles.

When this method is applied to the entire dataset of the BG and BN fumaroles, i.e., from 1983 to 2014, the temperature estimations (Fig. 7a) range from 190 °C to 240 °C, and they show a continuous increasing trend during the 2005-2014 phase of ground acceleration. During this last period, the temperature increased by ~15 °C, from 217 °C ±3°C in 2003-2004, to 232 °C ±2 °C in 2013-2014.

The estimated *f* values increase with time, in agreement with the heating of the system (Fig. 7b). Both the estimated temperatures and *f* have a marked negative anomaly during the 1983-1984 seismic crisis, when ~16000 earthquakes occurred at CFc (Fig. 7c). These anomalies might have been caused by more oxidizing conditions in the gas equilibration zone

during the crisis, in which case the estimated temperature and *f* values would not have a physical meaning because we assumed redox conditions fixed by a hydrothermal buffer. Alternatively, they might have been caused by a real temperature decrease as a result of the input of liquid water in the Solfatara plume. This second scenario is more likely, because the thousands of earthquakes that occurred in 1983-1984, which were generally located close to Solfatara, would increase the rock permeability by creating new fractures, thus promoting seepage of colder surface waters into the hydrothermal reservoir, and its subsequent cooling. In the following period, from 1985 to 2003, the *f* values are scattered around 0, with most of the temperatures ranging from 200 °C to 220 °C. After 2003, and to date (2014), the computed *f* values show systematic positive values that indicate water removal by the condensation and heating of the system.

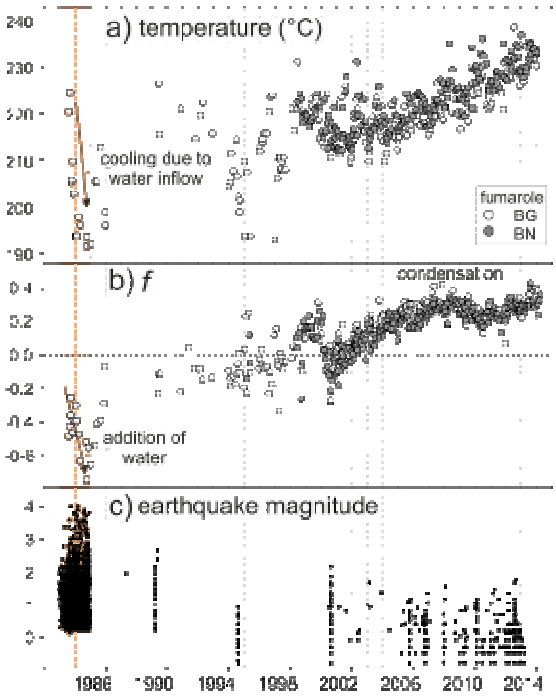

Figure 7. Temperature (a) and *f* values (b) inferred from thermodynamic computations within the H_2O-H_2-CO_2-CO gas system. The variable *f* refers to the fraction of the water removed (sign +) or added (sign -) during the transfer of the gas from the equilibration zone to the fumarole. Earthquake magnitudes are reported for comparison in (c) (data from D'Auria et al., 2011).

The estimated *f* values (Fig. 7b) show the same temporal pattern as the H_2 analytical values (Fig. 6d). This is not surprising, because the selection of fixed redox conditions imposes that the H_2/H_2O ratio is a function only of temperature, and deviations from equilibrium values are interpreted as removal (or addition) of water. If we do not assume the redox constraint but, e.g., that the measured H_2O is representative of the equilibrium values, we would estimate redox conditions that would become progressively more reducing over

time, which is not in agreement with the observed progressive decrease in CH_4 (Fig. 6b); this instead suggests the input of increasing amounts of oxidizing magmatic fluids in the deeper and hotter parts of the hydrothermal system.

3.3 Origin of the thermal anomaly

A first cause of the heating of the system would be the above-described increment in the flux of magmatic fluids that enter the hydrothermal system (Chiodini et al., 2012). Here, we investigate the changes in the H_2O/CO_2 ratio of the fluids released by the magma, as another possible cause of the 2005-2014 period of thermal anomaly. We have made use of the results of a recent study (Caliro et al., 2014) that used variations in the ratios among the most inert gas species measured at the Solfatara fumaroles (i.e., N_2, He, CO_2) to infer the main parameters (e.g., type of magma, pressure) that control the magma degassing processes from which these species mainly originate. The experimental data were compared with those simulated for a magma-degassing model of an isothermal open system involving (at different pressures: 100 to 300 MPa) the main types of melt compositions of CFc (i.e., trachybasalt, shoshonite, tephri-phonolite, trachyte). The results of this study show that the decrease in the pressure that governs the degassing of trachybasaltic magma might well explain the observed trends, and in particular, the decrease of the N_2/He ratio because N_2 has a solubility that is lower than He (Caliro et al., 2014).

The N_2/He ratio changed from ~700-800 in 1989, when the analysis of He was started, to ~200 in 2012-2014, showing a spectacular decreasing trend that is similar to that of the deflation during 1985-2004 (Fig. 8a). To estimate the correlation between these two processes, the data were fitted to an exponential decay model using the least absolute residual method. The results show that the time constants of the two trends are the same at the 95% confidence interval (10.3-10.6 years, 8.3-11.4 years, for the N_2/He and deformation, respectively). This co-incidence supports the concept of a common process to explain the observed variations. The process is most likely the depressurization of the deep parts of the systems, as concluded from recent independent studies of the geodetic and geochemical data. According to Amoruso et al. (2014a), the 1985-2004 deflation of CFc was due to a pressure decrease within a stationary deformation source (i.e., Fig. 5, PTE), while the N_2/He trend has been explained by a depressurizing magma degassing process (Caliro et al., 2014).

It is worth noting that the highest correlation between the geochemical signal and the ground deformation was found by moving the N_2/He ratio back by 900 days (Fig. 8a, inset), a delay that is larger than that estimated for the CH_4-based geoindicators (i.e., ~200 days; see

above), which indicates that the N_2/He ratio is controlled by a process that occurs below the hydrothermal system, and which furnishes another independent clue as to the magmatic origin of the signal.

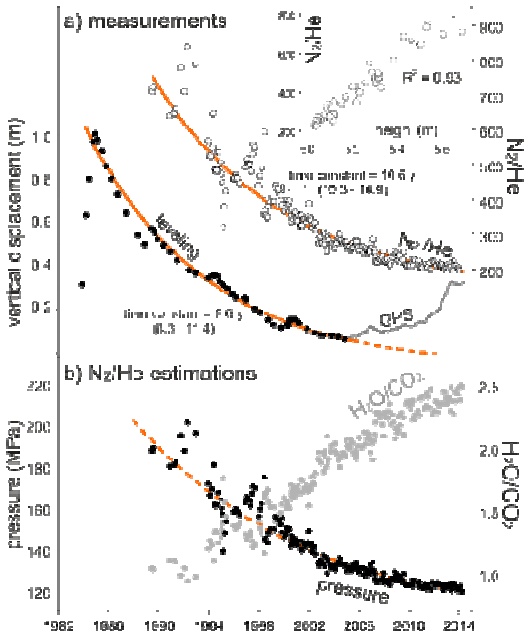

Figure 8. Geochemical indicators and ground deformation between 1982 and 2014. (a) Measured N_2/He ratio (BG fumarole) and maximum vertical ground displacement measured at CFc by optical leveling (black dots) and CGPS (data from Del Gaudio et al., 2010; De Martino et al., 2014). The exponential decay curve of the vertical height refers to the leveling data from 1985 to 2004. Inset: the N_2/He ratio plotted against the maximum height registered 900 days before. (b) H_2O/CO_2 ratio and pressure simulated for magmatic fluids released during an open-system degassing process (inferred from the measured N_2/He fumarolic ratios, see text).

From each measurement of the N_2/He ratio, we computed the corresponding pressure and H_2O/CO_2 ratio of the gas released from the magma (Fig. 8b), by comparison of the observed values with the data simulated in Caliro et al. (2014). Among the different models, we chose simulation with a H_2O/CO_2 molar ratio of 1 in the first separated gas phase, and an initial pressure of 200 MPa (see Caliro et al., 2014, for further details). Note that this arbitrary choice of the initial conditions, which for instance would roughly correspond to a depth of ~8 km assuming lithostatic control of the fluid pressure, affects the absolute values of the pressure and the H_2O/CO_2 ratio, but does not significantly affect the inferred degassing trends, because these mainly depend on the different solubilities of the gas species in the trachybasaltic melt. Inspection of the chronogram (Fig. 8b) shows that the magma degassing pressure would have decreased from 200 MPa to 120 MPa following an exponential decay trend, which matches well with an overpressure relaxation scenario; i.e., the system reached the maximum overpressure during the 1982-84 crisis, and since that time, it has tended to a baric equilibrium condition with the confining pressure.

Based on the mutual relationship between the ground deformation and the pressure of the magma degassing (Fig. 8), we hypothesize a top-down process of depressurization of the magmatic system that is possibly controlled by the permeability of the cover of the PTE, through which the pressure excess is released by fluid transfer to the shallower parts of CFc.

The correlation between the ground deformation and the N_2/He ratio, and the derived pressure trend of the magma degassing process, disappeared during the 2005-2014 period of accelerating uplift and heating of the system. It is worth noting that the magmatic fluids would have become progressively richer in steam concurrent with the depressurization, as indicated by the simulated H_2O/CO_2 ratio that almost doubled from 2000 (Fig. 8b). Steam has a much higher enthalpy than CO_2, and this energy can be transferred easily to the rock through condensation, to contribute to rock deformation.

3.4 Heating of the system and ground deformations

Considering the measured flux of CO_2 as constant ($FLUX_{CO2}$ ~1500 t/d), the total amount of steam that was condensed from 2003 to 2014 in the shallower part of the Solfatara gas plume (Fig. 4) was ~3.5 $\times 10^9$ kg, as result of the product $FLUX_{CO2} \times f \times (H_2O/CO_2)_{eq}$, integrated over the entire period. The corresponding total amount of heat released by this condensation was ~6.2 $\times 10^{12}$ kJ (i.e., with the latent heat of the steam condensation of ~1840 kJ/kg at the estimated average temperature of ~225 °C). This is an appreciable amount of energy, which would produce a 5 °C heat increase in a mass of ~1.25 $\times 10^{12}$ kg of rock, which corresponds to a volume of 0.625 km^3 (with a density of 2000 kg/m^3). On the assumption of a volumetric expansion coefficient of 30 $\times 10^{-6}$ /°C, the corresponding volume increase would be of ~0.94 $\times 10^5$ m^3; i.e., of the same order of magnitude as the volumetric expansion computed from ground deformation data by Amoruso et al. (2014b) for the shallower deformation source (PS in Fig. 4) for the period 2006-2013.

Similar, and possibly more intense, processes of heating, condensation and rock deformation will affect the deeper parts of the hydrothermal system, and probably also the magmatic gas zone (Fig. 4). Furthermore the effect of heating on ground deformation should be larger than that associated with the sole thermal expansion as suggested by the results of thermal techniques, and in particular steam injection, which are used in the oil industry for heavy-oil exploitation (e.g., Dusseault and Collins, 2008). The steam injection and the associated latent heat release will have three major effects: rock temperature increase, which in turn deforms the media through thermal expansion, thermally-induced shear dilation

(Dusseault, 2011), the associated ground deformation of which is remarkably large, and enhancement of fluid-flow permeability.

At CFc, the ongoing process of heating might be one of the main causes of the 2005-2014 accelerating process of ground deformation, because: (i) the mechanical strength of the products of the shallow layers of CFc (Neapolitan Yellow Tuff) strongly decreases with thermal stressing (Heap et al., 2014), (ii) increasing amounts of magmatic gas are entering into the system (see Chiodini et al., 2012: Fig. 4c), and (iii) the magmatic gases have a progressively higher enthalpy, due to the increase in the H_2O/CO_2 ratio.

More generally, the enrichment in water with respect to CO_2 will affect the fluids released by any process of magma depressurization, because it is controlled by the different solubilities of these two species in the melt. For any caldera, either during its ascent or during a steady passive degassing period (Girona et al., 2014), the magma will depressurize and release increasing amounts of steam that will heat the system, generating signs of long duration in the deformation patterns. The repetition of such episodes and the related heating phases might be one of the mechanisms that can explain long-term unrest cycles observed at calderas. Finally, the heating might bring the system to pre-eruptive conditions causing the weakness of the rocks which cover the magma bodies.

5. Conclusions

Campi Flegrei caldera is sited in the densely inhabited metropolitan area of Naples, and over the last few decades, it has given clear signs of unrest, which have included ground deformation, earthquakes, and variations in hydrothermal activity. The last main bradyseism episode (1982-1984) was followed by slow subsidence, which was interrupted by a few minor episodes of uplift, which lasted until 2005. Then a new inflation period started with an accelerating trend, and reached maximum vertical displacement in June 2014 (of 23 cm). To investigate the causes of this new unrest at CFc, we compared long time series of fumarolic compositions that were systematically collected at Solfatara from 1983 to 2014 with the ground deformation data, with impressive correlations shown between these two independent datasets.

An important characteristic of the hydrothermal system that feeds the fumarolic activity is its vertical gas plume that is 1.5 km to 2.0 km long, for which we show for the first time an evident *Vs* tomographic image. This vertical plume is the shallower part of a complex hydrothermal system that is composed of a zone at ~4 km in depth of magmatic gas accumulation, and a zone at ~2 km in depth where magmatic gases mix with and vaporize

meteoric liquid, to create the gas plume. A possible reason for the remarkable correspondence between these fumarolic compositions and the geophysical signals is the presence of this subterranean gas plume. This represents an efficient way for the transfer of fluids to the fumarolic discharges, while allowing the gas to maintain some signatures from the deeper zones of the system, the zones which are, at the same time, the sources of the CFc ground deformation.

These comparisons between the fumarolic compositions and the ground deformation suggest that two processes contribute to the ongoing CFc unrest:

1) Transient episodes of gas pressurization that are accompanied by fluid transfer from the deep magmatic gas zone to the shallower parts of the hydrothermal system, which trigger the short-term uplifting episodes;

2) A long-term process of heating of the system that causes (or contributes to) the 10-year-long pattern of accelerating ground deformation.

While the first of these processes has already been highlighted by recent investigations (Chiodini et al., 2012; D'Auria et al., 2011), the heating of the system by condensation as potentially the main factor involved in the control of the recent CFc dynamics is a possibility that has never been considered previously. The occurrence of this heating is suggested both by an evident increase in the hydrothermal activity at the surface and by the compositional variations of the fumarole gases that indicate both a temperature increase (i.e., increase in fumarolic CO and H_2, decrease in CH_4) and the occurrence of condensation processes within the hydrothermal system. The observed changes in the geochemical parameters occur simultaneously with the acceleration of the ground deformation.

The main reason for this phase of heating is an increase in the flux of magmatic steam, which following the 1983-84 bradyseism, might have been favored by a permeability increase in the cover of the magmatic zone and by the depressurization of the deep gas reservoir. As CO_2 has lower solubility than H_2O, the magma depressurization first produced the CO_2 exsolution during the major uplift stages, which then in the following stage caused a change toward more H_2O-rich compositions of the fluids released by the magma. The H_2O transferred as steam in the hydrothermal system can efficiently deform the rock.

To date, inversion of the CFc deformation data has been based on isothermal models that have neglected the thermal induced effects, which conversely might represent one of the

main processes in the recent deformation history of CFc. Coupled non-isothermal thermal-hydrologic-mechanical models, together with magma degassing simulations, and geochemical interpretation of fumarolic compositions can substantially improve our understanding of the trigger mechanisms of unrest at CFc, and in general, at any active caldera.

Acknowledgements

The authors thank J.B. Lowenstern and C. Werner for their com-ments that helped to improve the manuscript. This study has benefited from funding provided by the MEDiterranean SUpersite Volcanoes FP7 project (grant number 308665) and by the Italian Presidenza del Consiglio dei Ministri – Dipartimento della Pro-tezione Civile (DPC). This paper does not necessarily represent DPC official opinion and policies.

References

Aiuppa, A., Tamburello, G., Di Napoli, R., Cardellini, C., Chiodini, G., Giudice, G., Grassa, F., Pedone, M., 2013. First observations of the fumarolic gas output from a restless caldera: Implications for the current period of unrest (2005-2013) at Campi Flegrei. Geochemistry Geophysics Geosystems 14, 4153-4169, doi:10.1002/ggge.20261.

Amoruso, A., Crescentini, L., Sabbetta, I., 2014a. Paired deformation sources of the Campi Flegrei caldera (Italy) required by recent (1980-2010) deformation history. J. Geophys Res. 119, doi:10.1002/2013JB010392.

Amoruso, A., Crescentini, L., Sabbetta, I., De Martino, P., Obrizzo, F., Tammaro, U., 2014b. Clues to the cause of the 2011-2013 Campi Flegrei caldera unrest, Italy, from cGPS data. Geophys. Res. Lett., doi: 10.1002/2014GL059539.

Barberi, F., Corrado, G., Innocenti, F., Luongo, G., 1984. Phlegrean Fields 1982– 1984: Brief chronicle of a volcano emergency in a densely populated area. Bull. Volcanol. 47, 175- 185.

Battaglia, J., Zollo, A., Virieux, J., Dello Iacono, D., 2008. Merging active and passive data sets in travel-time tomography: The case study of Campi Flegrei caldera (southern Italy). Geophysical Prospecting 56 (4), 555-573, doi:10.1111/j.1365-2478.2007.00687.x.

Bruno, P.P.G., Ricciardi, G.P., Petrillo, Z., Di Fiore, V., Troiano, A., Chiodini, G., 2007. Geophysical and hydrogeological experiments from a shallow hydrothermal system at Solfatara Volcano, Campi Flegrei, Italy: Response to caldera unrest. J. Geophys Res. 112, B06201, doi:10.1029/2006JB004383.

Byrdina, S., Vandemeulebrouck, J., Cardellini, C., Legaza, A., Camerlynck, C., Chiodini, G., Lebourg, T., Gresse, M., Bascou, P., Motos, G., Carrier, A., Caliro, S., 2014. Relations between electrical resistivity, carbon dioxide flux, and self-potential in the shallow hydrothermal system of Solfatara (Phlegrean Fields, Italy). Submitted to JVGR.

Caliro, S., Chiodini, G., Moretti, R., Avino, R., Granieri, D., Russo, M., Fiebig, J., 2007. The origin of the fumaroles of La Solfatara (Campi Flegrei, South Italy). Geochimica et Cosmochimica Acta 71, 3040-3055, doi:10.1016/j.gca.2007.04.007.

Caliro, S., Chiodini, G., Paonita, A., 2014. Geochemical evidences of magma dynamics at Campi Flegrei (Italy). Geochim. Cosmochim. Acta 132, 1-15, doi:10.1016/j.gca.2014.01.021.

Chiodini, G., 2009. CO_2/CH_4 ratio in fumaroles a powerful tool to detect magma degassing episodes at quiescent volcanoes. Geophys. Res. Lett. 36, L02302, doi:10.1029/2008GL036347.

Chiodini, G., Avino, R., Caliro, S., Minopoli, C., 2011. Temperature and pressure gas geoindicators at the Solfatara fumaroles (Campi Flegrei). Ann. Geophys. 54, doi: 10.4401/ag-5002.

Chiodini, G., Brombach, T., Caliaro, S., Cardellini, C., Marini, L., Dietrich, V., 2002. Geochemical indicators of possible ongoing volcanic unrest at Nisyros Island (Greece). Geophysical Research Letters 29, no.16, 14.

Chiodini, G., Caliro, S., Cardellini, C., Granieri, D., Avino, R., Baldini, A., Donnini, M., Minopoli, C., 2010. Long-term variations of the Campi Flegrei, Italy, volcanic system as revealed by the monitoring of hydrothermal activity. J. Geophys. Res 11, doi:10.1029/2008JB006258.

Chiodini, G., Caliro, S., De Martino, P., Avino, R., Gherardi, F., 2012. Early signals of new volcanic unrest at Campi Flegrei caldera? Insights from geochemical data and physical simulations. Geology 40, 943-946, doi: 10.1130/G33251.1.

Chiodini, G., Cioni, R., 1989. Gas geobarometry for hydrothermal systems and its application to some Italian geothermal areas. Applied Geochemistry 4, 465-472.

Chiodini, G., Cioni, R., Magro, G., Marini, L., Panichi, C., Raco, B., Russo, M., 1996. Chemical and isotopic variations of Bocca Grande fumarole (Solfatara volcano, Phlegrean Fields). Acta Vulcanol. 8, 129–138.

Chiodini, G., Frondini, F., Cardellini, C., Granieri, D., Marini, L., Ventura, G., 2001. CO_2 degassing and energy release at Solfatara volcano, Campi Flegrei, Italy. J. Geophys. Res. 106, 16213-16221.

Chiodini, G., Marini, L., 1998. Hydrothermal gas equilibria: The H_2O-H_2-CO_2-CO-CH_4 system. Geochim. Cosmochim. Acta 62, 2673-2687.

Chiodini, G., Todesco, M., Caliro, S., Del Gaudio, C., Macedonio, G., Russo, M., 2003. Magma degassing as a trigger of bradyseismic events; the case of Phlegrean Fields (Italy). Geophysical Research Letters 30, 1434, doi:10.1029/2002GL016790.

Cioni, R., Corazza, E., Fratta, M., Guidi, M., Magro, G., Marini, L., 1989. Geochemical precursors at Solfatara Volcano, Pozzuoli (Italy), in: Latter, J.H. (Ed.), Volcanic Hazard. Springer Verlag, Berlin, pp. 384-398.

Cioni, R., Corazza, E., Marini, L., 1984. The gas/steam ratio as indicator of heat transfer at the Solfatara fumaroles, Phlegraean Fields (Italy). Bull. Volcanol. 47, 295-302.

D'Amore, F., and Panichi, C., 1980. Evaluation of deep temperatures in hydrothermal systems by
new gas geothermometer, Geochim. Cosmochim. Acta, 44, 549-556.

D'Auria, L., Giudicepietro, F., Aquino, I., Borriello, G., Del Gaudio, C., Lo Bascio, D., Martini, M., Ricciardi, G.P., Ricciolino, P., Ricco, C., 2011. Repeated fluid-transfer episodes as a mechanism for the recent dynamics of Campi Flegrei Caldera (1989-2010). J. Geophys Res. 116, no. B4, B04313, doi: 10.1029/2010JB007837.

D'Auria L., Giudicepietro F., Martini M. and Lanari R. (2012) The 4D imaging of the source of ground deformation at Campi Flegrei caldera (southern Italy). Journal of Geophysical Research, v.117, B08209, doi:10.1029/2012JB009181

De Martino, P., Tammaro, U., Obrizo, F., 2014. GPS time series at Campi Flegrei caldera (2000-2013). Annals of Geophysics 57, S0213, doi:10.4401/ag-6431.

De Siena, L., Del Pezzo, E., Bianco, F., 2010. Seismic attenuation imaging of Campi Flegrei: evidence of gas reservoirs, hydrothermal basins, and feeding systems. J. Geophys. Res. 115, B09312, doi:10.1029/2009JB006938.

Del Gaudio, C., Aquino, I., Ricciardi, G.P., Ricco, C., Scandone, R., 2010. Unrest episodes at Campi Flegrei: A reconstruction of vertical ground movements during 1905–2009. J. Volcanol. Geotherm. Res. 195(1), 48-56, doi:10.1016/j.jvolgeores.2010.05.014.

Di Vito, M.A., Isaia, R., Orsi, G., Southon, J., De Vita, S., D'Antonio, M., Pappalardo, L., Piochi, M., 1999. Volcanism and deformation since 12,000 years at the Campi Flegrei caldera (Italy). J. Volcanol. Geotherm. Res. 91, 221-246.

Dzurisin, D., Wicks, C.W., Poland, M.P., 2012. History of surface displacements at the Yellowstone caldera, Wyoming, from leveling surveys and InSAR observations, 1923-2008. US Geological Survey Professional Paper, (1788), 1-68.

Dusseault, M.B., 2011. Geomechanical Challenges in Petroleum Reservoir Exploitation. KSCE Journal of Civil Engineering 15(4), 669-678, doi:10.1007/s12205-011-0007-5.

Dusseault, M.B., Collins, P.M., 2008. Geomechanics Effects in Thermal Processes. CSEG Recorder, June 2008, 20-23.

Dvorak, J.J., Mastrolorenzo, G., 1991. The mechanisms of Recent vertical crustal movements in Campi Flegrei Caldera, southern Italy. Spec. Pap. Geol. Soc. Am. 263, 47.

Giberti, G., Yven, B., Zamora, M., Vanorio, T., 2006. Database on laboratory measured data on physical properties of rocks of Campi Flegrei volcanic area (Italy), in: Zollo, A., Capuano, P., Corciulo, M (Ed.), Geophysical exploration of the Campi Flegrei (southern Italy) caldera's interiors: data, methods and results.

Giggenbach, W.F., 1980. Geothermal gas equilibria. Geochim. Cosmochim. Acta 44, 2021-2032.

Giggenbach, W. F., 1997. Relative importance of thermodynamic and kinetic processes in governing the chemical and isotopic composition of carbon gases in high-heatflow sedimentary basins. Geochim. Cosmochim. Acta 61, 3763–3785.

Girona, T., Costa, F., Newhall, C., Taisne, B., 2014. On depressurization of volcanic magma reservoirs by passive degassing, J. Geophys. Res. Solid Earth, doi: 10.1002/2014JB011368.

Gottsmann, J., Marti, J., (Eds.), 2008. Caldera volcanism: Analysis, modelling and response. Dev. Volcanol. 10.

Heap, M.J., Baud, P., Meredith, P.G., Vinciguerra, S., Reuschlé, T., 2014. The permeability and elastic moduli of tuff from Campi Flegrei, Italy: implications for ground deformation modelling. Solid Earth 5, 1-20, doi:10.5194/se-5-1-2014.

Hill, D.P., 2006. Unrest in Long Valley Caldera, California, 1978-2004. Geol. Soc. Spec. Publ. 269, 1-24.

Legaz, A., Vandemeulebrouck, J., Revil, A., Kemna, A., Hurst, A.W., Reeves, R., Papasin, R., 2009. A case study of resistivity and self-potential signatures of hydrothermal instabilities,

Inferno Crater Lake, Waimangu, New Zealand. Geophys. Res. Letters 36, L12306, doi:10.1029/2009GL037573.

Lowenstern, J.B., Smith, R.B., Hill, D.P., 2006. Monitoring super-volcanoes: Geophysical and geochemical signals at Yellowstone and other large caldera systems. Philos. Trans. R. Soc. A 364, 2055-2072.

Morhange, C., Marriner, N., Laborel, J., Micol, T., Oberlin, C., 2006. Rapid sea-level movements and noneruptive crustal deformations in the Phlegrean Fields caldera, Italy. Geology 43, 93-96.

Newhall, C.G., Dzurisin, D., 1988. Historical unrest at large calderas of the world. U.S. Geol. Surv. Bull., 1855-1108.

Orsi, G., Di Vito, M.A., Isaia, R., 2004. Volcanic hazard assessment at the restless Campi Flegrei caldera. Bull. Volcanol. 66, 514-530.

Parks, M.M., Biggs, J., England, P., Mather, T.A., Nomikou, P., Palamartchouk, K., Papanikolaou, X., Paradissis, D., Parsons, B., Pyle, D.M., Raptakis, C., Zacharis, V., 2012. Evolution of Santorini Volcano dominated by episodic and rapid fluxes of melt from depth. Nature Geoscience 5, 749-754.

Petrillo, Z., Chiodini, G., Mangiacapra, A., Caliro, S., Capuano, P., Russo, G., Cardellini, C., Avino, R., 2013. Defining a 3D physical model for the hydrothermal circulation at Campi Flegrei caldera (Italy). J. Volc. Geotherm. Res. 264, 172-182, doi:10.1016/j.jvolgeores.2013.08.008.

Pruess, K., 1991. TOUGH2 – A general purpose numerical simulator for multiphase fluid and heat flow. Lawrence Berkeley Lab. Report LBL 29400.

Rinaldi, A.P., Todesco, M., Bonafede, M., 2010. Hydrothermal instability and ground displacement at the Campi Flegrei caldera. Physics of The Earth and Planetary Interiors 178, 155-161, doi:10.1016/j.pepi.2009.09.005.

Rosi, M., Sbrana, A., Principe, C., 1983. The Phlegrean Fields: Structural evolution, volcanic history and eruptive mechanisms. J. Volcanol. Geotherm. Res. 17, 273-288.

Todesco, M., 2009. Signals from the Campi Flegrei hydrothermal system: Role of a "magmatic" source of fluids. J. Geophys. Res. 114, B05201, doi:10.1029/2008JB006134.

Todesco, M., Chiodini, G., Macedonio, G., 2003. Monitoring and modelling hydrothermal fluid emission at La Solfatara (Phlegrean Fields, Italy); an interdisciplinary approach to the study of diffuse degassing. J. Volcanol. Geoth. Res. 125, 57-79.

Troise, C., De Natale, G., Kilburn, C.R.J., (Eds), 2006. Mechanisms of Activity and Unrest at Large Calderas. Spec. Publ. 269, Geol. Soc., London., pp. 1-24.

Vanorio, T., Virieux, J., Capuano, P., Russo, G., 2005. Three-dimensional seismic tomography from P wave and S wave microearthquake travel times and rock physics characterization of the Campi Flegrei Caldera. J. Geophys. Res. 110, B03201, doi:10.1029/2004JB003102.

Werner, C., Brantley, S., 2003. CO2 emissions from the Yellowstone volcanic system. Geochemistry Geophysics Geosystems 4, 1061, doi:10.1029/2002GC000473.

Wicks, C.W., Thatcher, W., Dzurisin, D., Svarc, J., 2006. Uplift, thermal unrest and magma intrusion at Yellowstone caldera. Nature 440, 72-75.

Zohdy, A.A.R., Anderson, L., Muer, L., 1973. Resistivity, self - potential, and induced - polarization surveys of a vapor - dominated geothermal system. Geophysics 38, 1130-1144.

Zollo, A., Capuano, P., Corciulo, M., (Eds.), 2006. Geophysical exploration of the Campi Flegrei (Southern Italy) Caldera interiors: Data, methods and results, Doppiavoce, Napoli, Italy.

Solfatara fumaroles analyses (1983-2014)

Analytical methods

For determination of major gas species, fumarolic gases were collected in evacuated flasks containing a 4N NaOH "caustic" solution (Giggenbach, 1975; Giggenbach and Goguel, 1989). In addition, condensed steam and non-condensable gases (dry gas) were sampled by flowing the fumarolic gases through a water-cooled condenser. Residual gases from the headspace of the caustic-bearing flasks were analyzed at the Geochemistry Laboratory of INGV-Osservatorio Vesuviano. Gas constituents were analyzed following the methods by Caliro et al. (2007). The chemical composition of residual gases was measured by gas chromatography through a unique injection on two molecular sieve columns (MS 5Å capillary, 30m x 0.53mm x 50· m; He and Ar as carrier gases) using thermal conductivity detectors (TCD) (analytical errors are < 3%). Carbon dioxide and sulfur species absorbed in the alkaline solution were analyzed after oxidation via H_2O_2, by acid-base titration and ion chromatography, respectively (analytical error ± 3%). Because of reaction in alkaline solution to form $COOH^-$ (Giggenbach and Matsuo, 1991), CO was analyzed on dry gas samples by means of gas-chromatographic separation with a MS 5 Å capillary, 30m x 0.53mm x 50· m column (He as carrier gas) coupled with a high-sensitivity reduced gas detector (HgO; detection limit 0.05 ppm; analytical error ± 3%).

Pure gases were used as standards for gas chromatographic analysis.

References

Caliro, S., Chiodini, G., Moretti, R., Avino, R., Granieri, D., Russo, M., Fiebig, J., 2007. The origin of the fumaroles of La Solfatara (Campi Flegrei, South Italy). Geochimica et Cosmochimica Acta 71, 3040-3055, doi:10.1016/j.gca.2007.04.007.

Giggenbach, W.F., 1975. A simple method for the collection and analysis of volcanic gas samples. Bull.Volcanol. 39, 132-145.

Giggenbach, W.F., Goguel, R.L., 1989. Collection and analysis of geothermal and volcanic water and gas discharges., Report No. CD 2401. Department of Scientific and Industrial Research. Chemistry Division. Petone, New Zealand.

Giggenbach, W.F., Matsuo, S., 1991. Evaluation of results from Second and Third IAVCEI field workshops on Volcanic gases, Mt. Usu, Japan, and White Island, New Zealand. Appl. Geochem. 6, 125-141.

Fumarole	date	T°C	H2O	CO2	H2S	Ar	N2	CH4	H2	He	CO	References
BG	12/06/1983	n.m.	840700	157100	1663	n.a.	303	23.9	245	n.a.	n.a.	a
BG	14/07/1983	n.m.	839000	158700	1739	n.a.	n.a.	n.a.	n.a.	n.a.	n.a.	a
BG	18/08/1983	157	844000	154000	1730	n.a.	343	28.2	240	n.a.	0.551	a
BG	11/09/1983	157	840000	158000	1810	n.a.	336	26.7	258	n.a.	0.64	a
BG	04/10/1983	157	844000	153700	1700	n.a.	343	25	240	n.a.	n.a.	a
BG	11/10/1983	n.m.	845000	153000	1779	n.a.	326	26.2	226	n.a.	0.339	a
BG	13/10/1983	156	828000	169000	1930	n.a.	378	27.2	241	n.a.	0.38	a
BG	14/10/1983	157	820800	176300	2041	n.a.	n.a.	n.a.	n.a.	n.a.	n.a.	a
BG	26/10/1983	n.m.	843800	153700	1751	n.a.	317	25	216	n.a.	n.a.	a
BG	03/11/1983	n.m.	836300	161100	1992	n.a.	337	26.1	233	n.a.	n.a.	a
BG	14/11/1983	n.m.	845000	153000	1880	n.a.	310	25	219	n.a.	0.391	a
BG	30/11/1983	156	846000	151900	1880	n.a.	323	25.1	216	n.a.	0.31	a
BG	06/12/1983	n.m.	851000	146600	1788	n.a.	355	27.4	230	n.a.	n.a.	a
BG	20/12/1983	n.m.	853000	144800	1705	n.a.	327	23.2	215	n.a.	n.a.	a
BG	11/01/1984	n.m.	847000	150500	1714	n.a.	329	22.9	222	n.a.	n.a.	a
BG	17/01/1984	157	851000	147000	1789	n.a.	313	21.8	212	n.a.	0.221	a
BG	26/01/1984	n.m.	846000	151700	1817	n.a.	323	22.8	214	n.a.	n.a.	a
BG	02/02/1984	n.m.	851000	146600	1667	n.a.	334	22.5	207	n.a.	n.a.	a
BG	03/02/1984	n.m.	850000	147700	1672	n.a.	305	21.6	210	n.a.	n.a.	a
BG	18/02/1984	n.m.	851000	146600	1818	n.a.	340	21.3	206	n.a.	n.a.	a
BG	21/02/1984	157	851000	147000	1760	n.a.	328	16.7	198	n.a.	0.221	a
BG	08/03/1984	n.m.	851000	146600	1667	n.a.	322	21.5	221	n.a.	n.a.	a
BG	15/03/1984	n.m.	848000	149700	1809	n.a.	310	20.4	196	n.a.	n.a.	a
BG	20/03/1984	n.m.	850000	147700	1770	n.a.	293	17	181	n.a.	n.a.	a
BG	23/03/1984	n.m.	857000	140900	1602	n.a.	350	19	190	n.a.	n.a.	a
BG	01/04/1984	n.m.	840000	157800	1664	n.a.	310	18.7	194	n.a.	n.a.	a
BG	03/04/1984	158	841000	156900	1700	n.a.	318	18.8	192	n.a.	0.27	a
BG	05/04/1984	n.m.	844000	153700	1774	n.a.	333	16.9	187	n.a.	n.a.	a
BG	09/04/1984	n.m.	848000	149900	1657	n.a.	333	16.4	181	n.a.	n.a.	a
BG	17/04/1984	n.m.	838000	159600	1863	n.a.	356	16.4	186	n.a.	n.a.	a
BG	26/04/1984	n.m.	843000	154600	1805	n.a.	366	15.1	181	n.a.	n.a.	a
BG	05/05/1984	n.m.	842000	155800	1659	n.a.	347	14.1	175	n.a.	n.a.	a
BG	10/05/1984	157	839000	159000	1800	n.a.	370	11.9	170	n.a.	0.259	a
BG	11/07/1984	n.m.	840000	167800	1562	n.a.	437	10.5	163	n.a.	n.a.	a
BG	20/09/1984	157	816000	181900	1210	n.a.	699	10.7	158	n.a.	0.201	a
BG	24/10/1984	157	811000	186900	1150	n.a.	794	10.6	146	n.a.	0.261	a
BG	24/10/1984	157	804000	194000	1200	n.a.	843	10.6	149	n.a.	0.29	a
BG	27/11/1984	156	805000	192900	1150	n.a.	819	10.1	150	n.a.	0.201	a
BG	24/01/1985	156	800000	198000	960	n.a.	860	10.2	153	n.a.	0.28	a
BG	13/03/1985	n.m.	785000	212800	1163	n.a.	907	9.7	169	n.a.	n.a.	a
BG	18/04/1985	157	786000	212000	1160	n.a.	877	12.8	186	n.a.	0.471	a
BG	02/06/1985	157	778000	220000	1090	n.a.	977	13.8	201	n.a.	0.491	a
BG	19/07/1985	n.m.	784000	213600	1080	n.a.	1013	13.4	188	n.a.	n.a.	a
BG	07/09/1985	157	777000	220900	1160	n.a.	1050	13.4	218	n.a.	0.62	a
BG	26/09/1985	157	777000	220500	1115	n.a.	1010	16.3	218	n.a.	n.a.	a
BG	22/11/1985	157	775000	222500	1127	n.a.	1037	16.3	205	n.a.	0.4	a
BG	18/12/1985	157	765000	232600	1135	n.a.	1072	18.3	237	n.a.	0.38	a
BG	26/02/1986	162	797400	200600	1037	n.a.	n.a.	n.a.	n.a.	n.a.	n.a.	a
BG	14/03/1986	162	785200	212600	1129	n.a.	n.a.	n.a.	n.a.	n.a.	n.a.	a
BG	24/04/1986	162	792100	205800	1102	n.a.	n.a.	n.a.	n.a.	n.a.	n.a.	a
BG	15/11/1986	162	793700	204200	1122	n.a.	n.a.	n.a.	n.a.	n.a.	n.a.	a
BG	24/04/1987	162	797100	200800	1132	n.a.	n.a.	n.a.	n.a.	n.a.	n.a.	a
BG	23/10/1987	162	812900	184800	1201	n.a.	840	31	240	n.a.	n.a.	a
BG	10/01/1988	162	807800	189800	1280	n.a.	810	30	260	n.a.	n.a.	a
BG	31/01/1988	162	812400	184400	1181	n.a.	807	30	262	n.a.	n.a.	a

Fumarole	date	T°C	H2O	CO2	H2S	Ar	N2	CH4	H2	He	CO	References
BG	01/02/1988	162	813500	184200	1204	n.a.	692	26	223	n.a.	n.a.	a
BG	23/03/1988	162	811800	186100	1129	n.a.	n.a.	n.a.	n.a.	n.a.	n.a.	a
BG	05/11/1988	162	812200	185600	1195	n.a.	n.a.	n.a.	n.a.	n.a.	n.a.	a
BG	06/01/1989	162	823700	174200	1110	n.a.	710	15.1	263	n.a.	n.a.	a
BG	15/06/1989	162	813400	184300	1138	n.a.	836	18.7	294	1.18	0.789	a
BG	29/06/1989	162	813400	184300	1138	n.a.	836	18.7	294	1.18	0.564	a
BG	15/07/1989	162	810800	186800	1135	n.a.	836	17.3	294	1.16	0.575	a
BG	09/11/1990	n.m.	790000	207800	1130	n.a.	761	20	274	1.19	0.756	a
BG	15/03/1991	n.m.	794400	203200	1149	n.a.	743	22	307	1.15	n.a.	a
BG	25/05/1991	n.m.	793800	203800	1202	n.a.	775	20	308	1.18	0.48	a
BG	21/10/1991	n.m.	806700	191000	1204	n.a.	731	24	298	0.94	0.57	a
BG	08/02/1992	162	814200	183300	1329	n.a.	723	25.6	316	1.02	0.64	a
BG	15/04/1992	n.m.	817300	180200	1338	n.a.	786	26.3	307	0.94	0.682	a
BG	12/09/1992	n.m.	829900	167700	1409	n.a.	610	24	293	n.a.	n.a.	a
BG	06/12/1992	n.m.	836300	161100	1526	n.a.	700	21.1	297	0.89	0.498	a
BG	29/12/1993	162	841500	156100	1429	n.a.	623	18.8	279	1.1	0.337	a
BG	03/02/1994	162	845900	151800	1329	n.a.	581	17.3	270	1.11	0.336	a
BG	01/03/1994	162	850400	147200	1380	n.a.	626	18.1	278	1.2	0.396	a
BG	10/04/1994	162	840500	157000	1372	n.a.	653	17	278	1.2	0.373	a
BG	11/05/1994	162	844600	153100	1270	n.a.	645	16.4	269	1	n.a.	a
BG	28/06/1994	162	839200	158500	1340	n.a.	596	19	285	1.23	0.47	a
BG	19/07/1994	162	841300	156600	1290	n.a.	579	19	279	1.21	0.36	a
BG	10/08/1994	162	837300	160500	1300	n.a.	599	18.8	281	1.24	0.32	a
BG	25/08/1994	n.m.	836900	160800	1250	n.a.	603	19.6	289	1.25	0.289	a
BG	16/09/1994	162	843600	154100	1292	n.a.	621	17.3	268	1.17	0.3	a
BG	13/10/1994	n.m.	838900	158700	1296	n.a.	639	17.9	284	1.2	n.a.	a
BG	26/12/1994	162	837500	160200	1223	n.a.	627	14.7	267	1.24	0.41	a
BG	21/01/1995	162	832500	165300	1201	n.a.	638	11.5	279	1.35	0.25	a
BG	04/02/1995	162	827500	170300	1196	n.a.	586	9.1	268	1.3	0.11	a
BG	09/03/1995	n.m.	832300	165700	1100	n.a.	526	7.8	252	1.65	0.391	a
BG	22/04/1995	164	825700	172300	1066	n.a.	578	7.6	270	1.53	0.104	a
BG	26/05/1995	n.m.	805200	192700	1196	n.a.	538	7.3	236	1.28	0.29	a
BG	27/12/1995	n.m.	816700	181000	1228	n.a.	646	13.6	296	1.41	0.51	a
BG	19/01/1996	162	807200	190500	1252	n.a.	689	14.1	307	1.5	0.52	a
BG	20/02/1996	162	810400	187300	1236	n.a.	704	15.7	332	1.5	0.541	a
BG	09/03/1996	162	826200	171500	1177	n.a.	656	14.8	311	1.42	0.51	a
BG	11/04/1996	162	825800	171900	1201	n.a.	679	15.6	310	1.48	0.53	a
BG	28/06/1996	162	826100	171400	1200	n.a.	650	15.2	311	1.46	0.53	a
BG	31/07/1996	162	816400	181600	1089	n.a.	674	15.5	279	n.a.	0.65	a
BG	30/08/1996	162	816700	184000	1190	n.a.	649	14.6	323	n.a.	0.72	a
BG	14/10/1996	162	829400	168500	1168	n.a.	653	15.5	308	n.a.	0.67	a
BG	28/12/1996	162	813200	184500	1222	n.a.	713	17.4	297	1.45	0.27	a
BG	31/01/1997	162	821900	175800	1221	n.a.	724	19.1	305	1.41	0.23	a
BG	28/02/1997	162	821400	176400	1189	n.a.	685	17.1	291	1.37	0.4	a
BG	25/03/1997	162	822300	175600	1119	n.a.	665	16.9	296	1.33	0.46	a
BG	18/04/1997	162	830900	166900	1191	n.a.	660	16.7	239	1.32	0.44	a
BG	03/05/1997	162	819000	178600	1267	n.a.	662	17.4	309	1.33	0.43	a
BG	21/05/1997	162	825200	172500	1271	n.a.	639	17.8	306	1.33	0.42	a
BG	18/06/1997	162	828800	169000	1180	n.a.	649	15.4	303	1.23	0.43	a
BG	17/07/1997	162	826300	171400	1170	n.a.	663	15.3	293	1.19	0.45	a
BG	02/09/1997	162	827600	170100	1198	n.a.	670	15.4	298	1.22	0.41	a
BG	16/12/1997	162	823800	173800	1256	n.a.	620	24.4	365	1.41	n.a.	a
BG	26/01/1998	162	834900	162800	1290	n.a.	582	22.6	348	1.25	0.594	a
BG	10/03/1998	162	828400	169100	1390	n.a.	603	24.1	354	1.24	0.532	a
BG	28/05/1998	162	832300	165700	1060	n.a.	570	28	393	1.6	0.602	a

Fumarole	date	T°C	H2O	CO2	H2S	Ar	N2	CH4	H2	He	CO	References
BG	23/06/1998	164	837500	160000	1307	n.a.	664	31	442	1.12	0.788	a
BG	29/07/1998	160	834400	163300	1360	0.872	557	28.4	396	1.53	0.604	a
BG	20/08/1998	162	829600	168000	1370	0.544	574	30.3	426	1.63	0.624	a
BG	29/09/1998	162	837200	160400	1361	0.43	432	23	326	1.25	0.56	a
BG	15/10/1998	161.3	840500	157300	1293	0.466	435	23.7	322	1.15	0.543	a
BG	16/11/1998	160.6	845100	152500	1338	1.05	561	30	399	1.4	0.534	a
BG	16/12/1998	162	842300	155400	1347	0.564	514	29.9	392	1.31	0.552	a
BG	23/03/1999	161	843500	154000	1394	0.489	507	31.8	423	1.29	0.518	a
BG	29/04/1999	162	848400	149000	1454	0.567	541	35.1	436	1.23	0.577	a
BG	03/06/1999	162	848300	149200	1448	0.444	506	33.1	405	1.18	0.551	a
BG	03/08/1999	150	835500	161900	1487	0.58	536	30.8	424	1.26	0.566	a
BG	16/09/1999	150.7	852900	144600	1469	0.42	499	28.1	418	1.22	0.565	a
BG	19/10/1999	151.5	828300	168700	1776	0.61	568	31.8	503	1.48	0.57	a
BG	25/11/1999	155.8	854500	143000	1536	0.436	460	23.4	374	1.06	0.429	a
BG	03/01/2000	157.2	867400	130300	1289	0.364	412	19.1	395	1.13	0.377	a
BG	29/02/2000	154.2	837000	160500	1533	0.432	471	19.6	373	1.26	0.615	a
BG	24/03/2000	151	853900	144000	1147	0.479	444	18.3	342	1.15	0.403	a
BG	11/04/2000	157	855000	143100	1019	0.365	435	17.6	319	1.1	0.447	a
BG	17/05/2000	156.3	827100	170300	1557	0.439	480	19.9	358	1.24	0.684	a
BG	15/06/2000	153	841500	156300	1268	0.501	465	18.6	347	1.17	0.544	a
BG	06/07/2000	161.3	847700	149900	1289	n.a.	n.a.	n.a.	n.a.	n.a.	n.a.	a
BG	01/08/2000	160.3	845400	152300	1366	0.609	453	19.4	351	1.35	0.427	a
BG	22/08/2000	160.5	847300	150600	1244	0.392	460	19	254	1.28	0.396	a
BG	23/08/2000	160	840600	157200	1298	0.631	495	20.1	269	1.34	0.498	a
BG	26/08/2000	161.1	844000	153700	1381	0.328	417	17.8	317	1.2	0.495	a
BG	25/10/2000	160.3	846500	151300	1310	0.389	415	19.1	324	1.22	0.572	a
BG	20/11/2000	160.3	842900	155000	1256	0.406	455	19.7	330	1.28	0.45	a
BG	20/11/2000	161.7	845500	152300	1285	0.375	443	19.1	322	1.23	0.443	a
BG	21/12/2000	161.3	842600	155300	1254	0.429	445	18.7	335	1.29	0.43	a
BG	15/01/2001	158.3	843600	154200	1265	0.527	446	17.4	343	1.31	0.43	a
BG	25/01/2001	160.5	844300	153500	1225	0.532	439	17.1	358	1.3	0.427	a
BG	01/03/2001	161	826100	171500	1385	0.575	492	17.5	372	1.4	0.474	a
BG	07/03/2001	160.9	840900	157000	1218	0.423	409	14.6	304	1.17	0.424	a
BG	02/05/2001	159.9	840800	157000	1262	0.555	436	16	334	1.24	0.616	a
BG	11/05/2001	159.1	837600	160300	1249	0.409	433	16.5	356	1.34	0.493	a
BG	11/05/2001	159.9	841400	156400	1270	0.4	429	16.8	343	1.33	0.481	a
BG	22/05/2001	158.6	835000	162800	1299	0.389	447	17.7	357	1.38	0.498	a
BG	19/07/2001	157.2	842300	155500	1230	0.522	445	19.5	342	1.3	0.656	a
BG	11/08/2001	158	834900	162900	1287	0.499	456	20.6	351	1.33	0.476	a
BG	28/09/2001	158.8	836800	161100	1253	0.321	448	22.6	354	1.35	0.455	a
BG	25/10/2001	158.3	837300	160600	1222	0.496	430	22.1	327	1.26	0.453	a
BG	29/11/2001	159.8	838400	159400	1243	0.39	418	22.7	334	1.2	0.406	a
BG	13/12/2001	159.8	837000	160800	1285	0.425	431	22.3	332	1.24	0.423	a
BG	08/01/2002	160.2	842800	155000	1271	1.892	480	23.6	342	1.24	0.434	a
BG	04/02/2002	161	828400	169200	1404	0.459	448	22.4	374	1.32	0.498	a
BG	27/02/2002	159.6	838000	159800	1289	0.382	413	20.3	355	1.2	0.475	a
BG	14/03/2002	159.3	836700	161000	1389	0.421	424	20	372	1.25	0.551	a
BG	18/04/2002	158.8	826400	171100	1498	0.586	436	19.4	423	1.38	0.658	a
BG	23/04/2002	160	828700	168800	1485	0.461	438	19.2	424	1.39	0.585	a
BG	09/05/2002	160.1	850100	147900	1063	0.511	383	16.2	367	1.16	0.538	a
BG	20/06/2002	161.7	830700	166800	1449	0.821	454	18.8	401	1.36	0.67	a
BG	15/07/2002	160.6	831600	166000	1464	0.469	456	18.4	400	1.47	0.574	a
BG	24/09/2002	161.5	832300	165500	1391	0.398	420	17.3	351	1.49	0.517	a
BG	24/10/2002	160	833000	164700	1367	0.338	453	19.6	386	1.66	0.515	a
BG	19/11/2002	159.6	827600	170100	1316	0.51	472	19.9	376	1.63	0.495	a

Fumarole	date	T°C	H2O	CO2	H2S	Ar	N2	CH4	H2	He	CO	References
BG	16/01/2003	161.9	828800	168900	1323	0.579	479	22.2	402	1.75	0.433	a
BG	25/02/2003	160.8	834200	163500	1335	0.533	513	23.3	396	1.68	0.447	a
BG	19/03/2003	160.4	825000	172600	1356	0.457	490	23.5	410	1.81	0.522	a
BG	19/03/2003	160.4	825000	172600	1356	0.457	490	23.5	410	1.81	0.522	a
BG	14/04/2003	161.8	818400	179000	1441	0.697	563	25	452	1.88	0.619	a
BG	11/06/2003	160.3	821100	176500	1397	0.458	466	19.1	385	1.88	0.56	a
BG	24/06/2003	161.4	823800	173800	1394	0.432	482	19.8	398	1.62	0.564	a
BG	03/07/2003	161	827600	170100	1343	0.499	479	18.9	398	1.66	0.536	a
BG	06/08/2003	161.8	827000	170600	1390	0.61	501	19.3	436	1.77	0.669	a
BG	26/09/2003	162.2	821300	176200	1438	0.46	467	16.8	410	1.73	0.601	a
BG	10/10/2003	162.4	798200	199000	1629	0.5	555	19.4	485	2.11	0.635	a
BG	11/11/2003	163.6	821000	176500	1441	0.535	488	16.6	422	1.8	0.535	a
BG	28/11/2003	163.5	821900	175700	1400	0.549	465	16	407	1.78	0.651	a
BG	16/01/2004	163	815800	181700	1407	0.648	515	18.1	430	1.91	0.532	a
BG	06/02/2004	162.3	817300	180300	1360	0.52	483	17.6	408	1.87	0.461	a
BG	23/03/2004	163	812900	184600	1450	0.611	503	17.4	394	1.83	0.498	a
BG	28/04/2004	158.6	811900	185700	1333	0.465	519	19.4	410	1.82	0.558	a
BG	31/05/2004	161.8	813600	184000	1304	0.71	569	21	442	2.02	0.56	a
BG	18/06/2004	161.6	826100	171500	1323	0.768	550	20.2	424	1.85	0.533	a
BG	30/07/2004	162.6	814200	183400	1328	0.581	520	18.4	409	1.86	0.683	a
BG	30/07/2004	162.6	817300	180500	1111	0.574	530	18.5	419	1.91	0.672	a
BG	17/09/2004	163.3	826600	171000	1358	0.563	490	19.4	405	1.8	0.558	a
BG	21/10/2004	163.2	817900	179700	1337	0.42	505	20.4	412	1.81	0.542	a
BG	25/11/2004	162.9	811400	186200	1324	0.467	519	21.3	425	1.86	0.516	a
BG	23/12/2004	161.9	815200	182300	1357	0.554	527	21.8	431	2.07	0.538	a
BG	11/01/2005	163.3	816000	181600	1337	0.437	485	20.3	400	1.85	0.548	a
BG	11/01/2005	163.3	816900	180700	1345	0.614	513	21.3	423	1.96	0.545	a
BG	09/02/2005	160	819000	178700	1306	0.567	511	21.5	424	1.92	0.567	a
BG	22/03/2005	159.8	812600	184900	1378	0.698	524	22.5	455	2	0.591	a
BG	28/04/2005	156	819500	178000	1366	0.554	526	21.9	464	1.98	0.567	a
BG	09/05/2005	157	812500	185000	1440	0.364	506	21.5	453	1.91	0.57	a
BG	09/05/2005	159	819000	178500	1378	0.444	513	20.4	460	2.02	0.551	a
BG	13/06/2005	161.2	797300	200200	1312	0.51	535	21.6	500	2.09	0.739	a
BG	13/07/2005	159.4	817100	180400	1405	0.462	488	19.7	455	1.89	0.55	a
BG	02/08/2005	160.1	810500	186900	1470	1.012	534	19.9	476	1.95	0.627	a
BG	22/09/2005	160	820700	176800	1420	0.59	494	18.3	431	1.83	0.604	a
BG	06/10/2005	160.5	807000	190400	1472	0.698	532	19.4	468	1.89	0.624	a
BG	10/10/2005	152.4	798500	198800	1535	0.751	555	19.6	466	2	0.625	a
BG	10/10/2005	152.4	810300	187100	1444	0.718	542	19.2	475	1.99	0.588	a
BG	01/12/2005	155.7	798300	199000	1533	0.934	538	19.1	483	2.05	0.709	a
BG	09/01/2006	159.1	809100	188400	1462	0.443	485	17.7	453	1.94	0.658	a
BG	08/03/2006	162	796600	198400	1488	n.a.	n.a.	17.9	484	2.13	0.685	a
BG	13/03/2006	161.7	812400	185300	1355	0.579	505	17.6	454	1.91	0.619	a
BG	24/04/2006	163.3	804600	193000	1487	0.928	513	17.1	443	1.94	0.721	a
BG	22/05/2006	161.7	797300	200300	1365	0.576	508	17.4	464	2.09	0.649	a
BG	21/06/2006	163	801700	195900	1401	1.027	511	17.9	445	1.97	0.723	a
BG	21/07/2006	163	803000	194600	1370	0.929	510	17.5	452	2.01	0.737	a
BG	06/09/2006	160.9	803700	194100	1376	0.674	451	15.4	411	1.85	0.637	a
BG	27/09/2006	159.7	796300	201100	1520	0.635	533	18.6	488	2.15	0.665	a
BG	23/10/2006	162.3	798900	198600	1509	0.496	498	17.9	469	2.03	0.64	a
BG	27/10/2006	162.9	801300	196200	1456	0.472	499	17.5	449	1.97	0.635	a
BG	13/11/2006	162.1	810000	187500	1473	0.835	527	17.8	469	2.14	0.604	a
BG	14/12/2006	157.2	799100	198200	1675	0.751	546	18.9	472	2	0.608	a
BG	18/01/2007	162.2	804500	193200	1350	0.766	475	15.8	444	1.84	0.645	a
BG	16/02/2007	159.2	807000	190800	1280	0.745	476	13.5	431	1.68	0.603	a

Fumarole	date	T°C	H2O	CO2	H2S	Ar	N2	CH4	H2	He	CO	References
BG	12/03/2007	161.4	786300	211100	1549	1.332	573	13.9	527	2.24	0.735	a
BG	18/04/2007	160.1	779600	217600	1669	1.381	593	11.3	555	2.41	0.739	a
BG	08/05/2007	162.5	784900	212600	1516	0.893	525	8.9	504	2.27	0.789	a
BG	31/05/2007	158.7	781100	216400	1456	1.057	512	7.9	489	2.33	0.759	a
BG	07/06/2007	161.9	783600	214100	1492	0.464	450	7.2	439	2.03	0.742	a
BG	17/07/2007	161.3	777000	220400	1596	1.032	504	8.3	487	2.3	0.946	a
BG	10/09/2007	163.5	764500	232900	1642	1.106	524	10.7	479	2.32	0.877	a
BG	17/10/2007	162.9	770200	227300	1538	0.791	504	11.9	457	2.26	0.832	a
BG	08/11/2007	162	764400	232800	1535	2.729	669	15.9	559	2.86	0.805	a
BG	03/12/2007	161.6	770200	227300	1533	0.948	539	14.1	444	2.18	0.767	a
BG	10/01/2008	162.2	765200	232300	1545	0.89	536	14.7	471	2.45	0.99	a
BG	05/02/2008	160.5	765500	232000	1519	0.53	507	14.4	453	2.3	0.856	a
BG	11/02/2008	161.5	770000	227600	1496	0.582	494	14	432	2.19	0.831	a
BG	17/03/2008	162.5	772800	224700	1508	0.477	480	14.4	455	2.19	0.899	a
BG	02/04/2008	162.5	780200	217400	1480	0.801	475	14	428	2.1	0.947	a
BG	13/05/2008	164	769100	228300	1568	0.586	530	15.7	505	2.51	0.979	a
BG	11/06/2008	163	764800	232500	1623	0.935	555	15.6	512	2.64	0.978	a
BG	15/07/2008	160.3	766800	230500	1605	1.433	585	15	526	2.51	0.818	a
BG	17/09/2008	163	769000	229000	1490	0.822	505	13.3	463	2.27	0.885	b
BG	09/10/2008	163.7	772000	226000	1490	1.36	544	14	480	2.36	0.795	b
BG	17/11/2008	164.8	761000	237000	1500	0.818	540	15.2	483	2.15	0.845	b
BG	17/12/2008	162.7	774000	223000	1580	0.935	533	15.2	471	2.24	0.783	b
BG	15/01/2009	163.8	770000	227000	1580	0.673	492	14.2	433	2.01	0.726	b
BG	24/02/2009	163.1	768000	230000	1550	0.992	526	14.9	467	2.35	0.788	b
BG	10/03/2009	163.3	779000	218000	1530	1.15	503	13.9	430	2.1	0.762	b
BG	15/04/2009	163.5	767000	230000	1530	1.25	518	13.2	444	2.21	0.953	b
BG	15/05/2009	n.m.	775000	222000	1500	0.69	453	11.4	408	2.06	0.856	b
BG	22/06/2009	162.8	772000	225000	1490	0.759	544	12.9	492	2.41	0.801	b
BG	14/07/2009	163	765000	232000	1510	0.556	558	13.1	489	2.27	0.774	b
BG	23/09/2009	162	768000	230000	1640	0.608	520	12.3	477	2.46	1.1	b
BG	19/10/2009	162.3	759000	239000	1570	0.796	545	12.3	489	2.6	1.02	b
BG	24/11/2009	n.m.	753000	244000	1720	2.24	605	12.1	461	2.5	0.966	b
BG	21/12/2009	161.5	774000	224000	1380	0.871	512	11.2	446	2.4	0.813	b
BG	05/01/2010	163.3	765000	233000	1430	0.656	512	11.5	455	2.45	0.98	b
BG	23/02/2010	163.7	766000	231000	1310	0.472	526	12.5	458	2.43	0.96	b
BG	17/03/2010	164.2	765000	233000	1250	1.16	575	13.5	465	2.53	0.94	b
BG	14/04/2010	161.3	772000	225000	1310	0.6	540	13.5	454	2.55	1.07	b
BG	10/05/2010	n.m.	760000	238000	1410	0.516	527	13.8	453	2.53	1.04	b
BG	16/06/2010	162.7	772000	226000	1320	0.856	555	14.5	448	2.45	1.02	b
BG	09/07/2010	163.6	771000	227000	1150	0.626	508	13.7	412	2.28	1.09	b
BG	15/09/2010	n.m.	776000	222000	1130	0.548	521	14.8	431	2.36	0.827	b
BG	21/10/2010	163.6	762000	235000	1160	0.77	558	15.6	459	2.5	0.857	c
BG	29/11/2010	162	753000	245000	1260	0.676	536	14.8	464	2.61	0.969	c
BG	07/12/2010	162.5	765000	233000	1220	0.684	540	14.8	463	2.62	0.857	c
BG	20/01/2011	165.2	758000	240000	1290	0.48	489	13.7	437	2.41	0.9	c
BG	15/03/2011	162	762000	235000	1180	0.572	523	15.4	462	2.42	1.008	c
BG	02/05/2011	163.2	765000	232000	1170	0.625	529	16.2	474	2.49	0.976	c
BG	24/05/2011	163.6	757000	241000	1130	0.591	464	13.9	440	2.32	1.039	c
BG	10/06/2011	163	768000	230000	1010	0.695	515	15.8	471	2.52	0.975	c
BG	25/07/2011	163.9	772000	226000	1240	0.527	513	16.6	468	2.39	0.925	c
BG	12/09/2011	163.1	766000	231000	1280	0.5	457	15.4	430	2.32	0.937	c
BG	04/11/2011	162.4	763000	235000	1440	0.51	501	17.2	449	2.25	0.851	c
BG	29/11/2011	163	769000	229000	1280	0.403	416	14.3	383	1.9	1.12	c
BG	13/01/2012	160.8	758000	240000	1350	0.547	532	17.8	500	2.45	1.049	c
BG	31/01/2012	160.7	767000	231000	1310	0.45	481	15.8	455	2.19	1.098	c

Fumarole	date	T°C	H2O	CO2	H2S	Ar	N2	CH4	H2	He	CO	References
BG	01/03/2012	n.m.	759000	238000	1280	0.517	521	16.7	516	2.5	1.18	c
BG	19/04/2012	165.4	766000	232000	1270	0.514	484	14.1	502	2.2	1.048	c
BG	02/05/2012	164.1	764000	234000	1290	0.512	490	14.2	499	2.33	1.037	c
BG	05/06/2012	165	772000	226000	1420	0.515	470	12.8	502	2.21	1.122	c
BG	13/07/2012	162.5	757000	240000	1370	0.476	521	14	529	2.48	1.462	c
BG	23/08/2012	164.8	762000	236000	1350	0.453	489	12.9	503	2.31	1.05	c
BG	21/09/2012	n.m.	746000	252000	1250	0.449	485	13.2	507	2.44	1.174	c
BG	25/10/2012	163.9	757000	241000	1250	0.394	469	13	490	2.35	1.109	c
BG	09/11/2012	162.6	744000	253000	1250	0.487	460	12.7	439	1.96	1.073	c
BG	09/11/2012	162.6	754000	243000	1420	0.541	510	14.4	527	2.48	1.121	c
BG	13/12/2012	162.3	762000	236000	1370	0.465	465	13.8	480	2.2	1.279	c
BG	10/01/2013	163.3	768000	230000	1330	0.472	451	14	454	2.14	1.095	c
BG	05/02/2013	162.6	757000	241000	1360	0.429	481	15.2	490	2.36	1.042	c
BG	28/03/2013	n.m.	754000	243000	1440	0.419	468	15.3	480	2.26	1.099	c
BG	16/04/2013	161.7	758000	240000	1450	0.387	517	16.1	517	2.38	1.294	c
BG	28/05/2013	163.2	752000	246000	1480	0.449	499	15.5	536	2.56	1.18	c
BG	20/06/2013	165.3	756000	242000	1470	0.481	502	15.2	532	2.4	1.311	c
BG	26/07/2013	163.4	742000	255000	1560	0.858	539	15.7	564	2.44	1.413	c
BG	23/08/2013	164.5	737000	260000	1620	0.435	522	15.4	574	2.5	1.297	c
BG	23/09/2013	164.2	746000	251000	1420	0.386	457	13.9	519	2.19	1.303	c
BG	17/10/2013	165	733000	265000	1440	0.363	489	14.9	561	2.46	1.329	c
BG	27/11/2013	163.9	742000	255000	1590	0.562	527	15.9	593	2.63	1.349	c
BG	17/12/2013	162.5	739000	259000	1600	0.515	486	14.9	554	2.48	1.243	c
BG	27/01/2014	162.5	741000	256000	1480	0.538	490	15.9	557	2.37	1.291	c
BG	19/02/2014	163	750000	248000	1410	0.404	431	14.3	507	2.23	1.28	c
BG	20/03/2014	162.5	742000	255000	1480	0.405	462	15.1	524	2.37	1.272	c
BN	09/03/1995	n.m.	828300	169900	883	n.a.	547	5.4	272	0.92	0.41	a
BN	22/04/1995	146	826300	172000	818	n.a.	n.a.	n.a.	n.a.	n.a.	n.a.	a
BN	28/04/1995	n.m.	821300	176900	846	n.a.	587	5.3	263	1.47	0.17	a
BN	26/05/1995	n.m.	810100	188100	869	n.a.	609	7.7	255	1.42	0.3	a
BN	16/12/1997	n.m.	819300	178500	1040	n.a.	663	22.8	374	1.36	n.a.	a
BN	27/01/1998	149	821700	176000	1080	n.a.	669	23.4	381	1.41	n.a.	a
BN	28/05/1998	150	822900	175000	1090	0.5	595	25.7	393	1.55	0.664	a
BN	23/06/1998	154.3	827600	170300	1039	n.a.	614	24	379	1.01	0.686	a
BN	29/07/1998	153.5	828600	169200	1090	0.535	597	26.9	412	1.57	0.655	a
BN	20/08/1998	152.7	839600	158400	1040	0.47	566	26.2	396	1.5	n.a.	a
BN	15/10/1998	148.2	835800	162300	1013	0.459	473	22.2	336	1.27	0.574	a
BN	16/11/1998	146	850300	147900	602	0.792	645	30.8	446	1.58	0.515	a
BN	16/12/1998	147	834300	163400	1164	0.973	582	28.3	415	1.39	0.57	a
BN	15/01/1999	147.1	839300	158500	1164	0.81	545	31.4	416	1.36	0.524	a
BN	16/03/1999	146.7	837000	160500	1239	0.843	585	30.3	448	1.52	0.519	a
BN	23/03/1999	146.7	846200	151600	1106	0.593	537	28.6	421	1.49	0.51	a
BN	29/04/1999	145.2	852300	145500	1075	0.545	569	31.4	430	1.42	0.5	a
BN	03/06/1999	147	860600	137200	1075	0.484	552	30.2	412	1.28	0.496	a
BN	03/08/1999	145.5	852400	145300	1125	0.55	543	26.7	414	1.27	0.586	a
BN	16/09/1999	150.9	852700	145200	1081	0.45	509	24.7	404	1.21	0.535	a
BN	19/10/1999	147.3	850700	147200	1045	0.44	522	24.8	456	1.37	0.54	a
BN	25/11/1999	149.8	847800	149700	1220	0.573	578	24.8	468	1.33	0.469	a
BN	03/01/2000	149.4	854700	143100	1102	0.719	528	20.1	423	1.34	0.427	a
BN	24/03/2000	148.5	846800	151300	970	0.536	471	16.6	352	1.23	0.472	a
BN	11/04/2000	149.1	849900	148200	932	0.494	477	16.8	341	1.22	0.488	a
BN	17/05/2000	149.1	853600	144700	900	0.531	432	15.2	311	1.12	0.403	a
BN	15/06/2000	148	873000	125000	1100	0.47	466	16.7	331	1.25	0.434	a
BN	06/07/2000	144.8	846400	151600	1010	0.43	484	17.2	341	1.28	0.438	a
BN	01/08/2000	146.2	869000	129300	876	0.453	391	15.8	320	1.14	0.428	a

Fumarole	date	T°C	H2O	CO2	H2S	Ar	N2	CH4	H2	He	CO	References
BN	22/08/2000	146.6	837900	160200	1063	0.673	511	18.3	274	1.44	0.473	a
BN	23/08/2000	145.9	868200	130100	896	0.553	444	17.3	256	1.19	0.423	a
BN	26/08/2000	144.7	841200	156800	1043	0.424	445	16.1	326	1.23	0.501	a
BN	13/09/2000	146.2	845500	152500	1036	0.702	478	17.6	326	1.24	0.49	a
BN	13/09/2000	145.8	847900	150200	1007	0.582	451	16	312	1.18	0.549	a
BN	13/09/2000	146.5	843200	154900	1034	0.568	482	17.5	332	1.26	0.512	a
BN	13/09/2000	146.8	844000	154100	1026	0.759	463	16.7	305	1.16	0.462	a
BN	13/09/2000	145.9	847900	150200	997	0.71	463	16.7	326	1.23	0.519	a
BN	13/09/2000	144.6	855600	142700	940	0.469	402	15	237	1.08	0.469	a
BN	13/09/2000	146.2	851800	146400	964	0.644	440	15.8	298	1.15	0.498	a
BN	13/09/2000	145.3	861700	136500	921	0.518	398	14.4	280	1.06	0.457	a
BN	25/10/2000	146.8	842400	155700	1009	0.588	447	17.6	330	1.26	0.44	a
BN	25/10/2000	146.6	846900	151200	986	0.428	442	17.5	329	1.24	0.423	a
BN	25/10/2000	146.7	848900	149200	957	0.368	433	17.4	322	1.23	0.418	a
BN	25/10/2000	146.6	851100	147100	944	0.383	418	16.8	313	1.2	0.44	a
BN	25/10/2000	146.1	847200	150800	1014	0.499	453	17.9	332	1.21	0.44	a
BN	25/10/2000	146.3	851100	147000	999	0.426	445	17.9	342	1.3	0.44	a
BN	25/10/2000	145.7	855800	142400	945	0.336	407	16.5	319	1.18	0.44	a
BN	25/10/2000	146.1	848700	149400	965	0.461	439	17.6	336	1.24	0.48	a
BN	25/10/2000	146.2	852500	145700	954	0.411	411	16.4	319	1.22	0.468	a
BN	25/10/2000	146.5	849300	148800	985	0.433	442	17.6	335	1.26	0.44	a
BN	25/10/2000	146.5	851100	147100	944	0.427	429	16.9	330	1.22	0.44	a
BN	25/10/2000	146.3	850000	148100	954	0.415	444	17.8	342	1.25	0.44	a
BN	25/10/2000	146.5	845400	152700	988	0.531	453	18	338	1.27	0.44	a
BN	25/10/2000	146.8	842500	155600	982	0.566	475	18.7	349	1.32	0.44	a
BN	20/11/2000	147.3	846200	151900	963	0.41	461	17.3	323	1.25	0.455	a
BN	24/11/2000	145.8	847600	150400	935	0.32	588	18.9	350	1.33	0.477	a
BN	24/11/2000	145.7	848500	149700	952	0.422	439	16.5	317	1.2	0.451	a
BN	21/12/2000	147.8	860200	138100	885	0.368	417	15.3	313	1.21	0.432	a
BN	15/01/2001	147	873100	125200	890	0.415	401	14	310	1.17	0.348	a
BN	17/01/2001	146.1	837700	160300	993	0.473	465	15.7	366	1.33	n.a.	a
BN	25/01/2001	147.2	841300	156800	976	0.422	437	14.5	358	1.31	0.433	a
BN	01/03/2001	146.3	862400	136000	837	0.419	387	12.2	293	1.11	0.413	a
BN	07/03/2001	146	839900	158400	915	0.308	410	12.7	315	1.19	0.435	a
BN	02/05/2001	145.3	843000	155100	1012	0.387	449	15.1	350	1.33	0.567	a
BN	11/05/2001	145	837600	160500	986	0.395	463	15.6	342	1.32	0.588	a
BN	22/05/2001	144.9	838900	159200	998	0.445	448	15.4	333	1.31	0.478	a
BN	31/05/2001	149.9	839200	158900	994	0.5	472	16.4	344	1.32	0.647	a
BN	19/07/2001	144.1	835100	163000	970	0.465	462	17.6	355	1.36	0.728	a
BN	11/08/2001	146.5	839700	158400	991	0.439	460	17.7	350	1.33	0.463	a
BN	28/09/2001	145.3	838500	159500	987	0.392	460	19.4	351	1.34	0.485	a
BN	25/10/2001	145.6	843000	155200	923	0.373	428	18.6	321	1.14	0.448	a
BN	29/11/2001	146.8	847000	151200	925	0.584	429	19	318	1.19	0.422	a
BN	13/12/2001	148	834300	163800	1007	0.535	434	18.9	332	1.25	0.454	a
BN	08/01/2002	148	840000	158100	1049	0.548	440	19.8	339	1.25	0.482	a
BN	04/02/2002	148.9	829700	168200	1101	0.482	461	19.6	375	1.31	0.533	a
BN	27/02/2002	147.7	841400	156700	1019	0.415	419	16.3	346	1.2	0.553	a
BN	14/03/2002	145.7	838700	159300	1037	0.456	430	17.4	357	1.23	0.485	a
BN	18/04/2002	145.8	828600	169200	1218	0.729	456	16.4	409	1.35	0.83	a
BN	23/04/2002	146.6	838600	159300	1108	0.773	435	15.4	385	1.27	0.556	a
BN	09/05/2002	145.7	843900	154100	1051	0.802	425	14.6	378	1.26	0.607	a
BN	22/05/2002	145	826900	171000	1175	0.572	458	16	424	1.36	0.626	a
BN	22/05/2002	146.2	826600	171300	1162	0.572	460	16.1	420	1.43	0.627	a
BN	22/05/2002	146.1	806700	191000	1281	0.537	470	16.9	437	1.39	0.699	a
BN	22/05/2002	145.2	837500	160500	1093	0.393	400	14.3	370	1.23	0.587	a

Fumarole	date	T°C	H2O	CO2	H2S	Ar	N2	CH4	H2	He	CO	References
BN	22/05/2002	145.1	825700	172100	1163	0.569	460	16	421	1.42	0.63	a
BN	22/05/2002	146.4	827400	170500	1147	0.476	442	15.8	406	1.37	0.624	a
BN	22/05/2002	146	840000	158000	1079	0.46	427	14.8	390	1.31	0.578	a
BN	20/06/2002	147.7	829500	168500	1068	0.674	451	15.5	397	1.43	0.549	a
BN	15/07/2002	146.3	832100	165900	1073	0.444	446	14.7	389	1.43	0.642	a
BN	24/09/2002	147.7	836100	161900	1068	0.415	456	15.5	366	1.55	0.54	a
BN	24/10/2002	147.9	836000	162000	1023	0.425	463	16.8	381	1.67	0.539	a
BN	19/11/2002	147.7	829900	168300	943	0.479	414	15.1	328	1.42	0.529	a
BN	16/01/2003	148.1	837600	160400	1012	0.637	481	18.5	402	1.74	0.448	a
BN	16/01/2003	148	846600	151600	777	0.414	467	18.4	393	1.72	0.45	a
BN	25/02/2003	148.4	833200	164700	1026	0.571	520	20	399	1.74	0.512	a
BN	19/03/2003	146	833800	164200	1006	0.469	431	18.2	351	1.42	0.53	a
BN	14/04/2003	147.7	831300	166700	1043	0.404	472	17.9	363	1.54	0.531	a
BN	11/06/2003	147.5	832200	165800	1036	0.57	471	15.8	378	1.61	0.619	a
BN	24/06/2003	147	815900	182200	971	0.741	468	15.2	383	1.38	0.602	a
BN	06/08/2003	147.7	819800	178100	1125	0.653	481	15.5	403	1.64	0.748	a
BN	26/09/2003	142.7	825100	172900	1075	0.47	450	13.2	391	1.6	0.632	a
BN	10/10/2003	147.5	833400	164500	1060	0.495	471	13.4	400	1.62	0.53	a
BN	11/11/2003	148.4	833300	164600	1031	0.432	475	13.4	413	1.76	0.551	a
BN	28/11/2003	146.5	827400	170600	1022	0.481	480	13.8	415	1.76	0.593	a
BN	16/01/2004	145	832200	165900	863	0.527	467	14	387	1.75	0.546	a
BN	06/02/2004	147.2	821700	176500	847	0.441	461	13.7	386	1.68	0.513	a
BN	23/03/2004	148	825900	172000	999	0.473	511	15.1	397	1.79	0.515	a
BN	29/03/2004	148	822200	175800	1004	0.453	513	15.8	401	1.76	0.545	a
BN	28/04/2004	147.7	821800	176300	866	0.639	542	16.8	423	2.02	0.547	a
BN	31/05/2004	147.6	816500	181300	1034	0.673	572	18.1	443	1.96	0.607	a
BN	18/06/2004	147.4	821700	176100	1015	0.488	569	18.1	447	2.06	0.56	a
BN	30/07/2004	147.7	816900	181100	982	1.007	557	16.5	417	1.86	0.691	a
BN	17/09/2004	147.3	818800	179100	1016	1.08	528	16.7	424	1.91	0.627	a
BN	21/10/2004	147.6	809800	188000	1050	1.022	564	18.4	453	1.96	0.657	a
BN	25/11/2004	147.2	821000	176900	1013	0.99	539	17.8	433	1.85	0.554	a
BN	23/12/2004	147.1	829800	168300	982	0.421	426	14.8	370	1.67	0.542	a
BN	11/01/2005	148.2	831700	166400	941	0.969	491	16.4	393	1.78	0.541	a
BN	09/02/2005	148	824700	173300	978	0.548	508	18	421	1.82	0.597	a
BN	22/03/2005	142.3	826300	171600	1007	0.478	480	17.1	429	1.83	0.569	a
BN	28/04/2005	139.9	825900	172100	995	0.521	493	18	444	1.76	0.578	a
BN	09/05/2005	147	823700	174200	1042	0.512	499	17.1	453	1.85	0.585	a
BN	09/05/2005	147	824800	173100	1035	0.376	489	17	439	1.72	0.581	a
BN	13/06/2005	145.4	818300	179700	995	0.433	494	16.5	462	1.81	0.721	a
BN	13/07/2005	148.5	820100	177800	1070	0.562	464	15	435	1.77	0.601	a
BN	02/08/2005	147.1	820500	177400	1036	0.784	503	15.8	461	1.8	0.692	a
BN	22/09/2005	145	821000	177000	1071	0.531	476	14.7	422	1.75	0.667	a
BN	10/10/2005	135.2	834600	163400	962	0.444	474	15	420	1.72	0.567	a
BN	01/12/2005	142.2	823300	174600	1049	0.532	465	13.8	437	1.81	0.687	a
BN	09/01/2006	145	825000	173000	1011	0.381	441	13.3	418	1.75	0.626	a
BN	08/03/2006	144.6	817400	180500	1036	0.58	489	14	450	1.87	0.729	a
BN	24/04/2006	145.5	810600	187300	1097	1.288	521	13.6	447	1.96	0.744	a
BN	24/04/2006	145.5	813500	184500	1080	0.853	485	13.4	422	1.84	0.733	a
BN	22/05/2006	146.1	804900	193200	923	0.572	487	13.4	460	1.89	0.695	a
BN	21/06/2006	145	818600	179500	1011	0.859	486	13.9	436	1.88	0.71	a
BN	21/07/2006	145.2	812100	185900	1053	0.696	493	14.3	455	1.96	0.71	a
BN	06/09/2006	144.6	810600	187400	1026	0.67	500	14.2	462	1.98	0.7	a
BN	27/09/2006	143	805200	192700	1128	0.79	486	13.9	457	1.9	0.691	a
BN	23/10/2006	145.2	808100	189800	1132	0.777	497	14	454	1.94	0.613	a
BN	27/10/2006	144.7	812200	185700	1091	0.523	487	14.4	440	1.89	0.672	a

Fumarole	date	T°C	H2O	CO2	H2S	Ar	N2	CH4	H2	He	CO	References
BN	13/11/2006	144.7	831100	166900	1037	0.851	515	14.2	460	2.03	0.606	a
BN	14/12/2006	142.5	812800	185000	1204	0.733	511	14.3	445	1.82	0.6	a
BN	18/01/2007	144	808400	189600	1003	0.737	490	13.3	471	1.94	0.655	a
BN	16/02/2007	141.8	807300	190800	960	0.883	485	11.4	448	1.77	0.633	a
BN	12/03/2007	143.7	803600	194200	1157	1.237	536	11	490	2.04	0.714	a
BN	18/04/2007	142.6	802500	195300	1130	1.305	545	8.5	511	2.13	0.702	a
BN	08/05/2007	143.7	787400	210500	1103	0.909	506	7.2	489	2.11	0.815	a
BN	07/06/2007	144.5	797900	200100	1065	0.557	465	6.3	471	2.14	0.769	a
BN	17/07/2007	143	780600	217200	1173	1.149	498	6.5	481	2.18	0.951	a
BN	10/09/2007	145	780600	217200	1187	0.904	498	8.3	480	2.26	0.886	a
BN	17/10/2007	146	776600	221200	1098	0.937	548	10.8	478	2.3	0.831	a
BN	08/11/2007	144.6	773600	224200	1107	1.357	546	10.7	480	2.28	0.961	a
BN	03/12/2007	145.1	776300	221700	1094	0.838	499	11.2	437	2.08	0.813	a
BN	10/01/2008	n.m.	774700	223100	1115	1.067	552	12.3	481	2.28	0.922	a
BN	05/02/2008	144	780500	217400	1090	0.544	515	12.1	457	2.29	0.849	a
BN	17/03/2008	145	765900	232000	1130	0.739	527	12.5	493	2.29	0.991	a
BN	02/04/2008	145.6	786000	212000	1105	0.45	484	11.7	467	2.17	1.168	a
BN	13/05/2008	145.3	768700	229100	1177	0.734	548	12.8	525	2.49	0.989	a
BN	11/06/2008	146.2	772100	225700	1235	1.005	519	11.5	496	2.39	1.058	a
BN	15/07/2008	150.6	771800	226000	1177	1.445	553	11.1	512	2.41	0.933	a
BN	17/09/2008	146.9	770000	228000	1090	0.613	505	10.6	488	2.3	0.945	b
BN	09/10/2008	148.2	772000	226000	1110	1.13	538	11.2	502	2.39	0.943	b
BN	17/11/2008	145.5	779000	218000	1140	0.841	523	11.6	487	2.26	0.847	b
BN	17/12/2008	147.3	785000	213000	1100	0.914	489	11	452	2.03	0.829	b
BN	15/01/2009	146.5	782000	216000	1130	0.689	493	11.4	439	1.96	0.766	b
BN	24/02/2009	145.7	774000	223000	1160	1.48	570	12.1	493	2.37	0.858	b
BN	10/03/2009	145.2	777000	221000	1160	0.771	509	11.4	459	2.22	0.893	b
BN	25/03/2009	141	776000	222000	1140	0.357	491	11.3	456	2.14	0.768	b
BN	15/04/2009	145.2	778000	220000	1160	0.955	505	10.3	452	2.24	0.894	b
BN	15/05/2009	n.m.	788000	210000	1110	0.588	452	9	426	2	0.79	b
BN	22/06/2009	146	784000	214000	1100	0.618	506	9.4	472	2.34	0.89	b
BN	14/07/2009	145.9	773000	225000	1130	0.633	487	8.7	476	2.08	0.818	b
BN	28/09/2009	n.m.	777000	221000	1010	0.632	504	9.2	468	2.25	1.19	b
BN	19/10/2009	145	774000	224000	1110	0.871	532	9.3	482	2.41	1.05	b
BN	24/11/2009	n.m.	762000	236000	1090	0.957	548	9.5	477	2.48	1.01	b
BN	21/12/2009	145	766000	232000	1080	0.602	498	8.7	453	2.28	1.08	b
BN	05/01/2010	145.9	762000	236000	1100	0.777	510	8.9	460	2.37	1.13	b
BN	14/01/2010	145.5	776000	222000	926	0.843	524	9.1	465	2.41	1.03	b
BN	23/02/2010	145	788000	210000	873	0.674	513	9.2	450	2.38	0.956	b
BN	17/03/2010	145.2	781000	217000	911	0.963	522	9.6	448	2.34	0.956	b
BN	14/04/2010	146	777000	221000	1000	0.759	515	9.9	443	2.33	1.15	b
BN	10/05/2010	146.1	767000	231000	1010	0.78	542	10.9	462	2.44	1.31	b
BN	16/06/2010	146.2	757000	241000	1020	0.8	570	11.9	480	2.54	1.23	b
BN	15/09/2010	n.m.	779000	219000	847	0.607	534	11.8	461	2.44	0.92	b
BN	21/10/2010	146.5	773000	225000	872	1.13	566	12.1	458	2.4	0.925	c
BN	21/10/2010	146.5	781000	217000	843	0.672	491	11	428	2.18	0.892	c
BN	29/11/2010	145.2	777000	221000	933	0.657	503	10.7	448	2.38	0.964	c
BN	07/12/2010	144.5	775000	223000	926	0.721	581	12.1	510	2.74	0.966	c
BN	20/01/2011	147.2	780000	219000	946	0.633	485	10.1	446	2.37	0.897	c
BN	15/03/2011	145.3	767000	232000	902	0.642	503	11.3	463	2.38	1.063	c
BN	02/05/2011	145.6	767000	231000	836	0.612	495	11.3	467	2.4	1.067	c
BN	24/05/2011	145	765000	234000	839	0.642	479	11.1	443	2.38	1.04	c
BN	10/06/2011	146.7	776000	223000	798	0.36	479	11.3	455	2.31	0.927	c
BN	25/07/2011	146.8	783000	215000	913	0.504	474	11.7	449	2.28	0.984	c
BN	12/09/2011	146.5	783000	216000	895	0.543	472	12	438	2.16	1.187	c

Fumarole	date	T°C	H2O	CO2	H2S	Ar	N2	CH4	H2	He	CO	References
BN	04/11/2011	145.3	777000	221000	1030	0.478	493	12.8	457	2.34	0.983	c
BN	29/11/2011	144.9	777000	221000	969	0.452	479	12.7	457	2.21	1.102	c
BN	13/01/2012	143.2	770000	228000	994	0.894	516	12.6	486	2.27	1.001	c
BN	31/01/2012	144.2	774000	224000	1010	0.512	484	12	481	2.19	1.103	c
BN	01/03/2012	n.m.	755000	243000	1000	0.538	536	12.8	543	2.43	1.276	c
BN	19/04/2012	145.5	765000	233000	979	0.492	497	10.9	536	2.42	1.103	c
BN	02/05/2012	146.5	773000	225000	953	0.45	473	10.3	512	2.34	1.116	c
BN	05/06/2012	146.5	776000	222000	1060	0.402	501	10.4	521	2.18	1.117	c
BN	11/06/2012	n.m.	766000	232000	1020	0.796	513	10.2	517	2.28	n.a.	c
BN	13/07/2012	144.5	761000	237000	1030	0.471	471	9.3	488	2.24	1.299	c
BN	23/08/2012	146.6	768000	230000	1000	0.488	482	9.6	503	2.31	1.052	c
BN	20/09/2012	145	761000	237000	910	0.607	497	9.9	513	2.34	1.272	c
BN	21/09/2012	n.m.	783000	215000	877	0.511	481	9.6	499	2.3	1.088	c
BN	25/10/2012	143.5	759000	239000	916	0.419	455	9.5	480	2.26	1.123	c
BN	09/11/2012	144.8	764000	234000	1060	0.512	482	10.2	468	2.15	1.075	c
BN	09/11/2012	144.8	772000	226000	1010	0.482	464	9.6	482	2.17	1.035	c
BN	13/12/2012	144.2	759000	239000	1030	0.544	492	10.6	513	2.32	1.386	c
BN	10/01/2013	143.4	765000	233000	988	0.569	479	10.9	492	2.2	1.036	c
BN	05/02/2013	144	766000	232000	977	0.423	457	10.7	471	2.13	1.071	c
BN	28/03/2013	n.m.	765000	233000	1070	0.48	464	11.4	469	2.17	1.106	c
BN	16/04/2013	144.5	755000	243000	1110	0.535	530	12.4	519	2.35	1.357	c
BN	28/05/2013	144.6	765000	233000	1070	0.6	495	11.4	513	2.34	1.176	c
BN	20/06/2013	144.5	761000	237000	1080	0.497	499	11.2	524	2.33	1.296	c
BN	26/07/2013	145.6	738000	260000	1190	0.806	548	12	581	2.46	1.337	c
BN	23/08/2013	145.6	719000	279000	1320	0.541	552	12.1	606	2.58	1.486	c
BN	23/09/2013	145.4	759000	239000	1060	0.459	464	10.2	511	2.23	1.268	c
BN	17/10/2013	145	762000	236000	1030	0.448	451	9.9	506	2.15	1.218	c
BN	27/11/2013	144	756000	242000	1190	0.543	481	10.7	532	2.31	1.256	c
BN	17/12/2013	144.2	761000	236000	1290	0.499	457	10.3	511	2.21	1.185	c
BN	27/01/2014	142	774000	224000	945	0.839	458	10.1	486	2.1	1.18	c
BN	19/02/2014	142.6	748000	250000	1010	0.462	444	11	524	2.29	1.293	c
BN	20/03/2014	143.7	730000	268000	1060	0.326	461	11.4	533	2.4	1.334	c

Chemical compositions are in mmol/mol
n.a. not analyzed - n.m. not measured
a) Chiodini et al., 2010 and references therein
b) Chiodini et al., 2011
c) This work